

Stochasticity of Deterministic Gradient Descent: Large Learning Rate for Multiscale Objective Function

Lingkai Kong* and Molei Tao†

February 17, 2020

Abstract

This article suggests that deterministic Gradient Descent, which does not use any stochastic gradient approximation, can still exhibit stochastic behaviors. In particular, it shows that if the objective function exhibit multiscale behaviors, then in a large learning rate regime which only resolves the macroscopic but not the microscopic details of the objective, the deterministic GD dynamics can become chaotic and convergent not to a local minimizer but to a statistical distribution. A sufficient condition is also established for approximating this long-time statistical limit by a rescaled Gibbs distribution. Both theoretical and numerical demonstrations are provided, and the theoretical part relies on the construction of a stochastic map that uses bounded noise (as opposed to discretized diffusions).

Keywords: deterministic gradient descent, large learning rate, multiscale objective function, statistical limit, rescaled Gibbs distribution, Li-Yorke chaos, bounded noise, escape from microscopic minima and microscopic minima

1 Introduction

Optimization is a central ingredient of machine learning. First-order optimization algorithms, for instance, are particularly popular for deep learning tasks due to their scalabilities to high-dimensional problems, because they employ gradient but not higher-order information of objective functions for iteratively approximating minimizers.

Among first-order methods, arguably the most used is gradient descent method (GD), or rather one of its variants, stochastic gradient descent method (SGD). Designed for objective functions that sum a large amount of terms, which for instance can originate from big data, SGD introduces a randomization mechanism of gradient subsampling to improve the scalability of GD (e.g., Zhang [2004], Moulines and Bach [2011], Roux et al. [2012]). Consequently, the iteration of SGD, unlike GD, is not deterministic even when it is started at a fixed initial condition. In fact, if one fixes the learning rate (LR) in SGD, the iteration does not converge to a

*School of Mathematics, University of Science and Technology of China

†School of Mathematics, Georgia Institute of Technology. mtao@gatech.edu

local minimizer like in the case of GD; instead, it converges to a statistical distribution with variance controlled by the LR (e.g., Borkar and Mitter [1999], Mandt et al. [2017], Li et al. [2017]). Diminishing LR was thus proposed to ensure that SGD remains as an optimization algorithm [Robbins and Monro, 1951]. On the other hand, more recent perspectives include that the noise in SGD may actually facilitate escapes from bad local minima and improve generalization (see Sec.1.2 and references therein). In addition, non-diminishing LRs often correspond to faster computations, and therefore are of practical relevance¹. Meanwhile, GD does not need the LR to be small in order to reduce the stochasticity, although in practices the LR is often chosen small enough to fully resolve the landscape of the objective, corresponding to a stability upper bound of $1/L$ under the common L -smooth assumption of the objective function.

This article considers deterministic GD with fixed large LR, based on the conventional belief that it makes optimization more efficient than small LR GD does. The goal is to understand if large LR will work, and if yes, in what sense. We will show that in a specific and yet not too restrictive setup, if the LR becomes large enough (but not arbitrarily large), GD does not converge to a local minimum but instead a statistical distribution. This behavior bares significant similarities with SGD, including (under reasonable assumptions):

- starting with a deterministic initial condition, the empirical distribution of GD iterates converges to a specific statistical distribution, which is not Dirac but almost a rescaled Gibbs distribution, just like SGD;
- starting an ensemble of initial conditions and evolving each one according to GD, the empirical distribution of the ensemble, collected at the same number of iterations, again converges to the same almost Gibbs distribution as the number of iteration increases, also like SGD.

Their difference, albeit obvious, should also be emphasized:

- GD is deterministic, and the same constant initial condition will always lead to the same iterates. No filtration is involved, and unlike SGD the iteration is not a stochastic process.

In this sense, GD with large LR works in a statistical sense. One can obtain stochasticity without any algorithmic randomization! Whether this has implications on generalization is beyond the scope of this article, but large LR does provide a mechanism for escapes from local minima. We'll see that microscopic local minima can always be escaped, and sometimes macroscopic local minima too.

1.1 Main Results

How is stochasticity generated out of determinism? Here it is because of chaotic dynamics. To further explain, let us introduce our setup: consider objective function $f : \mathbb{R}^d \rightarrow \mathbb{R}$ defined through a macro-micro decomposition

$$f(x) := f_0(x) + f_{1,\epsilon}, \text{ where } f_{1,\epsilon} := \epsilon f_1\left(\frac{x}{\epsilon}\right),$$

¹Optimizing the LR is an important subarea but out of the scope of this paper; see e.g., Smith [2017] and references therein.

$0 < \epsilon \ll 1$, $f_0, f_1 \in \mathcal{C}^2(\mathbb{R}^d)$, and f_1 is a periodic function with a constant period $T \in \mathbb{R}^d$, i.e.,

$$f_1(x + T) = f_1(x), \forall x \in \mathbb{R}^d$$

Such objectives are multiscale functions exhibiting different behaviors over two scales, where f_0 dictates the macroscopic behavior and $f_{1,\epsilon}$ adds fine details of microscopic oscillations to it. See Fig.1.

Note although the length and height scales of $f_{1,\epsilon}$ are both $\mathcal{O}(\epsilon)$, much smaller than those of f_0 , ∇f_0 and $\nabla f_{1,\epsilon}$ are nevertheless both $\mathcal{O}(1)$, creating nonconvexity and a large number of local minima even if f_0 is (strongly) convex.

This class of f models objective landscapes that assume certain macroscopic shapes, but when zoomed-in exhibiting additional small-in- x & f fluctuations. Taking the loss function of a neural network as an example, our intuition is that if the training data is drawn from a distribution, the distribution itself could produce the dominant macroscopic part of the landscape (i.e., f_0), and noises in the training data will lead to $f_{1,\epsilon}$ which corresponds to small and localized perturbations to the loss. The remaining problem is, such perturbations may not be periodic. For this we note the theories in this paper do rely on periodicity (analogous to classical multiscale theories such as periodic homogenization (e.g., Pavliotis and Stuart [2008]), periodic averaging (e.g., Sanders et al. [2010]) and KAM theory (e.g., Moser [1973])), but our result (i.e. stochasticity) persists as numerically observed in problems with nonperiodic micro-scale behaviors (see Sec.3.2).

What will happen when gradient decent is applied to $f(x)$, following repeated applications of the map

$$\varphi(x) := x - \eta \nabla f(x) = x - \eta \nabla f_0(x) - \eta \nabla f_{1,\epsilon}(x)?$$

η is called the time step or learning rate, the latter will be used throughout this article.

It is well known that when $\eta \ll \epsilon$, GD converges to a local minimum (or a saddle, or in general a stationary point where $\nabla f = 0$). For $\eta \gg 1$, or more precisely when it exceeds $1/L$ for L -smooth f , the iteration generally blows up and does not converge. However, there is a regime inbetween corresponding to $\epsilon \lesssim \eta \ll 1$, and this is what we call large LR, because here η is too large to resolve the micro-scale (i.e., $f_{1,\epsilon}$, whose gradient has an $\mathcal{O}(\epsilon^{-1})$ Lipschitz constant).

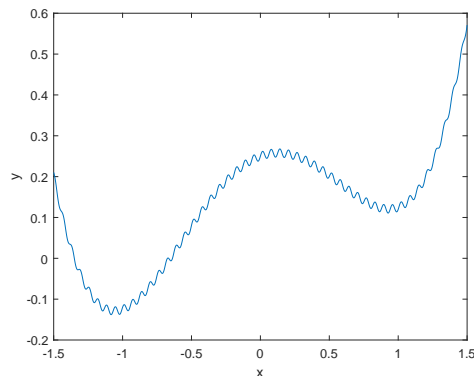


Figure 1: Graph of an example multi-scale function, $f(x) = \frac{1}{4}(x^2 - 1)^2 + \frac{x}{8} + \epsilon \sin\left(\frac{x}{\epsilon}\right)$, $\epsilon = 0.01$

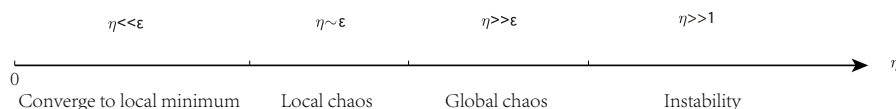


Figure 2: What happens as learning rate increases?

Fig.2 previews what happens over the spectrum of η values. The difference between ‘local chaos’ and ‘global chaos’ will be detailed in Sec. 2.3.1 and 2.3.2.

In fact, for the multiscale function f , one may prefer to find a ‘macroscopic’ local minimum created by f_0 , instead of being trapped at one of the numerous local minima created by f_1 , which could just be artifacts due to imperfection of training data. A small LR will not be able to do so, but we’ll see below that large LR in some sense is better at this: it will lead GD to converge to a distribution peaked at f_0 minimizer(s), despite that the iteration is based on the $\nabla f(x) = \nabla f_0(x) + \nabla f_1(x/\epsilon)$.

Our approach for demonstrating the ‘stochasticity’ of φ consists of three key ingredients: (i) construct another map $\hat{\varphi}$, which is a truly stochastic counterpart of φ , so that they share the same invariant distribution; (ii) find an approximation of the invariant distribution of $\hat{\varphi}$, namely rescaled Gibbs; (iii) establish conditions for φ iterations to generate deterministic chaotic dynamics, which provides a route of convergence to a statistical distribution.

More specifically, we define the stochastic map $\hat{\varphi}$ as

$$\hat{\varphi} : x \mapsto x - \eta \nabla f_0(x) + \eta \zeta,$$

where $\zeta = -\nabla f_1(U)$ for a uniform distributed random variable U on $\otimes_{i=1}^d [0, T_i]$, i.i.d. if $\hat{\varphi}$ is iterated. Then we have (note many of these conclusions persist under relaxed conditions in numerical experiments; see Sec.3).

Theorem 1 (informal version of Thm.4). *Fix η and let $\epsilon \rightarrow 0$. If φ has a family of nondegenerate² invariant distributions for $\{\epsilon_i\}_{i=1}^{\infty} \rightarrow 0$, this sequence of distributions converges to an invariant distribution of $\hat{\varphi}$.*

Theorem 2 (informal version of Lem.1, Thm.9 & Thm.5). *Suppose $f_0 \in \mathcal{C}^2$ is strongly convex and L -smooth, and $f_1 \in \mathcal{C}^1$ is periodic. Then for $\eta \leq C$ with some $C > 0$ independent of ϵ , $\hat{\varphi}$ has an unique invariant distribution, and its iteration converges exponentially fast to this distribution. Moreover, if the covariance matrix of $\zeta = -\nabla f_1(U)$ with uniform U is isotropic, i.e., $\sigma^2 I_d$, then the rescaled Gibbs distribution $\frac{1}{Z} \exp\left(-\frac{2f_0(x)}{\eta\sigma^2}\right) dx$ is an $\mathcal{O}(\eta^2)$ approximation of it.*

Theorem 3 (informal version of Thm.7). *Suppose $f_0, f_1 \in \mathcal{C}^1(\mathbb{R})$ and f_1 is periodic. If f_0 has a stationary point and f_1 is not a constant, then $\exists C > 0$, s.t. when $\eta > C\epsilon$, the iteration of φ with f is chaotic.*

In addition, we will establish period doubling, which is a common route of transition from regular dynamics to chaos as η increases [Alligood et al., 1997]. We will also establish and approximate a positive Lyapunov exponent of φ in the large LR regime, and this is strongly correlated with chaotic dynamics [Lyapunov, 1992].

The reason that we investigate chaos is the following. Although general theories are not unified yet, it is widely accepted that chaotic systems are often ergodic (on ergodic foliations), meaning the temporal average of an observable along any orbit (starting from the same foliation)

²By ‘nondegenerate’, we require the distribution to have Lipschitz continuous density. Invariant distribution of φ always exists; an example is a Dirac distribution concentrated at any stationary point of f . See Rmk.3.

converges, as the time horizon goes to infinity, to the spatial average of that observable over an invariant distribution (e.g., Eckmann and Ruelle [1985], Young [1998], Ott [2002]). Moreover, many chaotic systems are also mixing (see e.g., Ott [2002]), which implies that if one starts with an ensemble of initial conditions and evolves each one of them by the deterministic GD map, then the whole ensemble converges to the (ergodic) invariant distribution.

Therefore, our last step in establishing stochasticity of GD is to show that the deterministic φ map becomes chaotic for large η . This way, in most situations it is also ergodic and the assumption of Theorem 1 is satisfied, allowing us to demonstrate and quantify the stochastic behavior of deterministic GD. Note that we also know that if f_0 has multiple minima and associated potential wells, then GD can have stochastic behaviors with non-unique statistics (see Remark 12, 9 and Section C.4). For mixing we do not have a proof but only numerical evidence (see section 3.1 and C.3), but we note that (i) since mixing implies ergodicity, our necessary conditions for ergodicity are also necessary conditions for mixing, and (ii) proving mixing of deterministic dynamics is difficult, and only several examples have been well understood; see e.g., Sinai [1970], Ornstein and Weiss [1973].

Remark 1. For these reasons, we clarify that the theory in this paper does not quantify the speed of convergence of deterministic GD (φ) to its long time statistical limit. It is only shown that the stochastic map $\hat{\varphi}$ converges to its statistical limit exponentially fast for strongly-convex f_0 , and the deterministic map φ shares the same statistical limit with $\hat{\varphi}$.

1.2 Related Work

(S)GD is one of the most popular optimizing algorithms for deep learning, not only because of its practical performances, but also due to extensive and profound theoretical observations that it both optimizes well (e.g., Lee et al. [2016], Jin et al. [2017], Du et al. [2019b,a], Allen-Zhu et al. [2019b]) and generalizes well (e.g., Neyshabur et al. [2015], Bartlett et al. [2017], Golowich et al. [2018], Dziugaite and Roy [2017], Arora et al. [2018], Li and Liang [2018], Li et al. [2018], Wei et al. [2019], Allen-Zhu et al. [2019a], Neyshabur and Li [2019], Cao and Gu [2020], E et al. [2020]).

However, to the best of our knowledge, there are not yet many results that systematically study the effects of large learning rates from a general optimization perspective. Jastrzębski et al. [2017] argues that large LR makes GD more likely to avoid sharp minima (we also note whether sharp minima correspond to worse generalization is questionable, e.g., Dinh et al. [2017]). Another result is Li et al. [2019b], which suggests that large LR resists noises from data. In addition, Smith and Topin [2019] associates large LR with faster training of neural networks. To relate to our work, note it can be argued from one of our results (namely the rescaled Gibbs statistical limit) that LR smooths out shallow and narrow local minima, which are likely created by noisy data. Therefore, it is consistent with Li et al. [2019b] and complementary to Jastrzębski et al. [2017] and Smith and Topin [2019]. At the same time, one of our contributions is the demonstration that this smoothing effect can be derandomized and completely achieved by deterministic GD.

Another related result is Draxler et al. [2018], which suggests that few substantial barriers appear in the loss landscape of neural networks, and this type of landscape fits our model, in

which most potential wells are microscopic (i.e., shallow and narrow).

In addition, since we demonstrate stochasticity purely created by large LR, the technique of Polyak-Ruppert averaging [Polyak and Juditsky, 1992] for reducing the variance and accelerating the convergence of SGD is expected to remain effective, even when no stochastic gradient or minibatch approximation is used. A systematic study of this possibility, however, is beyond the scope of this article. Also, our result is consistent with the classical decreasing LR treatment for SGD (e.g., Robbins and Monro [1951]) in two senses: (i) in the large LR regime, reducing LR yields smaller variance (eqn.1); (ii) once the LR drops below the chaos threshold, GD simply converges to a local minimum (no more variance).

1.2.1 On the insufficiency of modified equation

Recently there has been an interesting line of research in which discrete algorithms are studied through their continuum limits (e.g., Su et al. [2014], Wibisono et al. [2016], Liu et al. [2017], Franca et al. [2018], Ma et al. [2019], Tao and Ohsawa [2020]); these limits, however, correspond to a small LR (denoted by η) regime.

It is possible to slightly extend this regime by writing down a limiting ODE that includes additional correction terms (e.g., Shi et al. [2018], Li et al. [2019a], Kovachki and Stuart [2019]). The classical notion for systematically doing so is backward error analysis and modified equation (e.g., Hairer et al. [2006]). For example, the GD map φ can be formally approximated, via an application of the modified equation theory, by $\dot{x} = -\nabla \tilde{f}(x)$, where the modified loss

$$\tilde{f}(x) = f(x) + \frac{\eta}{4} \|\nabla f(x)\|_2^2 + \mathcal{O}(\eta^2).$$

While informative, this result does not help us understand the large LR regime. In fact, due to that $f(x) = f_0(x) + \epsilon f_1(x/\epsilon)$, when $\eta \geq C\epsilon$ for some $C > 0$, the formal series expansion used in modified equation does not converge (see Appendix), which renders it inapplicable.

This paper thus develops a completely different framework to understand the large LR regime.

2 Theory

Proofs and additional remarks are provided in Appendix B.

2.1 Connecting the deterministic map and the stochastic map

Here we will build connections between the stochastic map $\hat{\varphi}$ and the deterministic map φ . The intuition is that as $\epsilon \rightarrow 0$ they share the same long-time behavior. In the following discussion, we fix the learning rate η , and in order to show the dependence of φ on ϵ , we write it as φ_ϵ explicitly in this section.

Theorem 4 (convergence of the deterministic map to the stochastic map). *Let $\hat{\varphi}(X) := X - \eta \nabla f_0(X) + \eta \zeta$ where ζ is a random variable defined as $\zeta := -\nabla f_1(U)$, with U being a uniform-distributed random variable on $\otimes_{i=1}^d [0, T_i]$, i.i.d. if $\hat{\varphi}$ is iterated. $T = (T_1, \dots, T_d)$ is the period*

of f_1 . Denote by $\hat{\varphi}_\# \mu$ and $\varphi_{\epsilon\#} \mu$ the pushforwards of density μ , i.e., respectively the density of $\hat{\varphi}(X)$ and $\varphi_\epsilon(X)$ with $X \sim \mu$.

Assume there exist a subset of probability density functions in \mathbb{R}^d , $\mathcal{F} \subset L^2(\mathbb{R}^d) \cap \mathcal{P}(\mathbb{R}^d)$, and a subset $\mathcal{E} \subset \mathbb{R}$ with $0 \in \bar{\mathcal{E}} \setminus \mathcal{E}$, that satisfy:

1. Every function in \mathcal{F} is uniformly Lipschitz continuous, with Lipschitz constant bounded above by a universal constant $L_{\mathcal{F}}$.
2. $\forall \epsilon \in \mathcal{E}$, $\varphi_{\epsilon\#} \mathcal{F} \subset \mathcal{F}$. $\hat{\varphi}_\# \mathcal{F} \subset \mathcal{F}$.
3. $\varphi_{\epsilon\#} : \mathcal{F} \rightarrow \mathcal{F}$ is uniformly equicontinuous according to $\epsilon \in \mathcal{E}$ under $\|\cdot\|_2$. $\hat{\varphi}_\# : \mathcal{F} \rightarrow \mathcal{F}$ is continuous under $\|\cdot\|_2$.
4. $\varphi_{\epsilon\#}$ has fixed points in \mathcal{F} , $\forall \epsilon \in \mathcal{E}$. Denote the set of its fixed points as $\Omega_\epsilon = \{\nu_\epsilon \in \mathcal{F} : \varphi_{\epsilon\#} \nu_\epsilon = \nu_\epsilon\}$. And $\hat{\varphi}$ has fix points in \mathcal{F} , denoted by $\hat{\Omega}$ as the non-empty set of fix points of $\hat{\varphi}_\#$ in $\bar{\mathcal{F}}$ (the closure is under norm $\|\cdot\|_2$).

Then if we let $\{\epsilon_i\}_{i=1}^\infty \subset \mathcal{E}$ be a sequence with 0 limit satisfying $\forall i, \Omega_{\epsilon_i} \neq \emptyset$, then for any sequence of arbitrarily chosen $\nu_i \in \Omega_{\epsilon_i}$, the sequence $\{\nu_i\}_{i=1}^\infty$ has limit points and all the limit points are in $\hat{\Omega}$.

Remark 2. Here the space $(L^2, \|\cdot\|_2)$ can be replaced by any Banach space, $(L^p, \|\cdot\|_p)$ with $1 \leq p \leq \infty$ for instance.

Remark 3. In this paper, we call invariant distributions with Lipschitz continuous densities to be nondegenerate. We only consider them because there are also degenerate invariant distributions, which correspond to Dirac distributions at stationary points of f . In fact, if one starts GD with initial condition that is any stationary point of f , GD won't exhibit any true stochasticity no matter how large the LR is. We avoid considering such a degenerate limiting distribution by excluding them from our function space.

2.2 The stochastic map: quantitative ergodicity

This section will show that, when f_0 is strongly convex, the stochastic map $\hat{\varphi}$ induces a Markov process that is geometric ergodic, meaning it converges exponentially fast to a unique invariant distribution. We will also show that when f_1 is isotropic, the invariant distribution can be approximated by a rescaled Gibbs distribution. As an additional remark, we also believe that rescaled Gibbs approximates the invariant distribution when f_0 is not strongly convex, even though no proof but only numerical evidence is provided (Sec.3.1); however, geometric ergodicity can be lost.

Lemma 1 (geometric ergodicity). *Consider $\hat{\varphi}(x) = x - \eta \nabla f_0(x) + \eta \zeta$, where ζ is a bounded random variable in \mathbb{R}^d with 0 mean, i.i.d. if $\hat{\varphi}$ is iterated. If f_0 is strongly convex, \mathcal{C}^2 and L -smooth, then there exists $\eta_0 \in \mathbb{R}^+$, such that when $\eta < \eta_0$, the map $X \mapsto \hat{\varphi}(X)$ has a unique invariant distribution and the iteration $\hat{\varphi}^{(n)}(X)$ converges (as $n \rightarrow \infty$) to the invariant distribution in Prokhorov metric exponentially fast for any initial condition.*

Lemma 2 (gradient estimate of rescaled Gibbs). *Let x_0 be the global minimizer of f_0 . If*

$$C_1 \|x - x_0\|^{k_1} < f_0(x) - f_0(x_0) < C_2 \|x - x_0\|^{k_2}, \quad \forall x \in \mathbb{R}^d,$$

Then we have, for X_0 following rescaled Gibbs (1),

$$\mathbb{E} \|\nabla f_0(X_0)\|_2^2 = \mathcal{O}(\eta^{2k_2 - 2 - \frac{1}{k_1}})$$

Proposition 1 (rescaled Gibbs nearly satisfies the invariance equation). *Suppose $f_0 \in C^1(\mathbb{R}^d)$ is L -smooth. Consider $\hat{\varphi}$ defined in Lemma 1. Suppose ζ is isotropic, i.e. with covariance matrix $\sigma^2 I_d$ for a scalar σ . Let X_0 be a random variable following rescaled Gibbs distribution*

$$X_0 \sim \frac{1}{Z} \exp\left(-\frac{2f_0(x)}{\eta\sigma^2}\right) dx \quad (1)$$

Then for any $h \in C^2$ with compact support, we have, for small enough η , that

$$\mathbb{E}h(\hat{\varphi}(X_0)) - \mathbb{E}h(X_0) = \mathcal{O}(\eta^3)$$

Remark 4. Note that strong convexity and L -smoothness of f_0 are sufficient to satisfy the condition of Lemma 2, but they may not be necessary. In fact, Prop. 1 is also correct for any f_0 that satisfies

$$C_1 \|x - x_0\|^{k_1} < f_0(x) - f_0(x_0) < C_2 \|x - x_0\|^{k_2},$$

where $2k_2 - 2 - \frac{1}{k_1} \geq 1$. Although we only proved that the rescaled Gibbs approximates the invariant distribution when f_0 is strongly convex functions, the fact that rescaled Gibbs nearly satisfies the invariance equation does not require strong convexity. In fact, we conjecture that rescaled Gibbs also approximates the invariant distribution for convex and even nonconvex f_0 . See numerics in Sec.3.1 ($f_0 = x^4/4$, with $k_1 = k_2 = 4$) and Appendix C.4 (nonconvex and multimodal f_0).

Theorem 5 (rescaled Gibbs is an approximation of the invariant distribution). *Denote by ρ_∞ the density of the unique invariant distribution of $\hat{\varphi}$, i.e., $L\rho_\infty = \rho_\infty$, then under the setup of Thm. 9 we have, in weak-* topology,*

$$\rho_\infty = \tilde{\rho} + \mathcal{O}(\eta^2) \quad (2)$$

where $\tilde{\rho}$ is rescaled Gibbs distribution with density $\tilde{\rho}(x) = \frac{1}{Z} \exp\left(-\frac{2f_0(x)}{\eta\sigma^2}\right)$.

2.3 Deterministic Map

Since we want to link the invariant distributions of the deterministic map and the stochastic map, the existence of nondegenerate invariant distribution of the deterministic map (which is important, see Rmk.3) should be understood, as well as the convergence towards it. The last part of Sec.1.1 discussed that chaos can usually provide these properties, but it is not guaranteed, and mathematical tools are still lacking. Thus, in previous theorems, such existence was assumed instead of being proved. We first present two counter examples to show that nondegenerate invariant distribution can actually be nonexistent.

1. In 1-dim, for a wide range of f_1 and ϵ , \exists a convex \mathcal{C}^2 f_0 and an η arbitrarily large, s.t. any orbit of φ is bounded, but the invariant distribution has to be a fixed point (Thm.10)
2. In 1-dim, for a wide range of f_0 and η , \exists a periodic \mathcal{C}^2 f_1 and an ϵ arbitrarily small, s.t. the invariant distribution has to be a fixed point (Thm.11)

Then we show GD iteration is chaotic when LR is large enough (for nondegenerate x_0).

2.3.1 Li-Yorke Chaos

In this section, we fix η in order to bound the small scale effect in simpler notations, and write the dependence of φ on ϵ explicitly. The main message is φ induces chaos in Li-Yorke sense. Note there are several definitions of chaos (e.g. Block and Coppel [2006], Devaney [2018], Li and Yorke [1975], and Aulbach and Kieninger [2001] is a review of their relations). We first quote Li-Yorke's celebrated theorem (Li and Yorke [1975]; see also Sharkovskii [Original 1962; Translated 1995]).

Theorem 6 (period three implies chaos). *Let J be an interval and let $F : J \rightarrow J$ be continuous. Assume there is a point $a \in J$ for which the points $b = F(a)$, $c = F^2(a)$ and $d = F^3(a)$, satisfy $d \leq a < b < c$ or $(d \geq a > b > c)$, then*

1. For any $k = 1, 2, \dots$, there is a periodic point in J having period k .
2. There is an uncountable set $S \subset J$ containing no periodic points, that satisfies:
 - (A) For every $p, q \in S$ with $p \neq q$, $\limsup_{n \rightarrow \infty} |F^n(p) - F^n(q)| > 0$ and $\liminf_{n \rightarrow \infty} |F^n(p) - F^n(q)| = 0$.
 - (B) For every $p \in S$ and periodic point $q \in J$, $\limsup_{n \rightarrow \infty} |F^n(p) - F^n(q)| > 0$.

Then we apply this tool to the GD map φ :

Theorem 7 (sufficient condition for deterministic GD to be chaotic). *Suppose $f_0, f_1 \in \mathcal{C}^1(\mathbb{R})$ and f_1 has period T . If $\exists x$ s.t. $\nabla f_0(x) = 0$ and f_1 is not a constant value function, then $\exists \epsilon_0$, s.t. when $\epsilon < \epsilon_0$, φ_ϵ induces chaotic dynamics in Li-Yorke sense.*

Remark 5. Li-Yorke theory is restricted to 1D and Thm.7 cannot easily generalize to multi-dim. Lyapunov exponent in Sec.2.3.3 however provides a hint and quantification for chaos in multi-dim.

Remark 6. The threshold ϵ_0 may be dependent on the stationary point x , and thus ϵ_0 obtained from an arbitrary x may not be the largest threshold under which chaos onsets.

Remark 7. The threshold ϵ_0 considered in this theorem is only for local chaos to happen. In fact, as the proof will show, only very weak conditions are needed because here chaos onsets due to that GD evolving within a microscopic potential well is a unimodal map. See also Sec.2.3.2.

However, as ϵ further decreases beyond the threshold, or equivalently as η increases, global chaos onsets shortly after. The idea is, when there is only local chaos but not a global one, the empirical distribution of iterations concentrates at a local minimum inside a microscopic well, but its variance grows as η increases. Shortly after, the distribution floods over the barriers of this microscopic well, and then local chaos transits into global chaos. Sec.2.3.3 will allow us to see that both local and global chaos happen when $\eta \sim \epsilon$.

2.3.2 Period Doubling

When η is small, each (local) minimizer of f corresponds to a stable fixed point of φ , which is thus also a periodic orbit of φ with period 1. As η increases, this point remains as a fixed point but will become unstable. Instead, the previously stable periodic orbit bifurcates into a stable periodic orbit with period 2, and the period similarly keeps doubling as η further increases. Eventually, the period becomes arbitrarily large before a finite value of η , as will be numerically illustrated in Sec.8. This phenomenon is known as period doubling, which is a common route to chaos (e.g., Alligood et al. [1997], Ott [2002]); after the appearance of arbitrarily large period, the system enters η regime that corresponds to chaotic dynamics.

We now explain how this relates to what we call global and local chaos, which are specific to our multiscale problem.

When $\eta \ll \epsilon$, we know GD converges to a local minimum of f corresponding to one of the many potential wells of created by f_1 . This is the non-interesting case.

When η approaches the same scale of ϵ , which is at the order of the width of microscopic potential wells of f_1 , the orbit is still trapped in a single microscopic potential well, but it starts making jumps within the well. In fact, restricted to any potential well, φ becomes a unimodal map (see e.g., Strogatz [2018]) and its dynamics is known to eventually become chaotic as η exceeds a critical value. This is where the period of a periodic orbit keeps on doubling and becomes arbitrarily large. The classical method for studying the invariant distribution of unimodal chaotic maps applies here (see e.g., Cvitanovic [2017]). This is the local chaos regime.

Even more interesting is the case when η gets even larger, large enough for the orbit to jump out of a single potential well created by f_1 and navigate the landscape of f_0 . This is what we call global chaos. For this, Thm.4 and 1 characterize the combined effect of chaos and global behavior of f_0 .

2.3.3 Lyapunov Exponent

Lyapunov exponent characterizes how near-by trajectories deviate exponentially with the evolution time. A positive exponent shows sensitive dependence on initial condition, is often understood as a lack of predictability in the system (due to a standard argument that initial condition is never measured accurately), and is commonly associated with chaos. Strictly speaking it is only a necessary condition for chaos (see e.g., Strogatz [2018] Chap 10.5), but it quantifies the strength of chaos.

Suppose $(x_0, x_1, \dots, x_n, \dots)$ is a trajectory of iterated map φ . Then the following measures the deviation of near-by orbits and thus defines the Lyapunov exponent:

$$\lambda(x_0) = \lim_{n \rightarrow \infty} \frac{1}{n} \sum_{i=0}^{n-1} \ln \|\nabla \varphi(x_i)\|_2 \quad (3)$$

This quantity is often independent of the initial condition (see e.g., Oseledec [1968]), and we will see that this is true in numerical experiments with GD. Moreover, we can quantitatively estimate λ :

Theorem 8 (approximate Lyapunov exponent of GD). *Suppose the deterministic map is ergodic, then the Lyapunov exponent of the deterministic map starting from x , denoted by $\lambda(x)$, satisfies*

$$\lambda(x) = m + \ln\left(\frac{\eta}{\epsilon}\right) + \mathcal{O}(\epsilon + \eta)$$

for which ϵ first goes to 0 and then η goes to 0. m is a constant given by

$$m = \frac{1}{|\Gamma|} \int_{\Gamma} \ln \|Hess f_1(y)\|_2 dy,$$

where the set $\Gamma = \otimes_i [0, T_i]$ and $|\Gamma|$ is its volume.

Remark 8. A necessary condition for chaos is a positive Lyapunov exponent. From the equation $\lambda(x) \approx m + \ln\left(\frac{\eta}{\epsilon}\right)$, we know chaos happens when $\eta > e^{-m}\epsilon$. This threshold (consistent with Thm.7) does not distinguish between local and global chaos, whose difference was hidden in the higher order term. One may ask why f_0 doesn't appear in m . The reason is, the microstructure creates both local and global chaos, not the macrostructure; in fact, since $L \ll 1/\epsilon$, L for the L -smooth f_0 gets absorbed in the high-order term in the proof.

3 Numerical Experiments

Additional results, including verifications of statements about chaos (period doubling & Lyapunov exponent estimation), as well as multidimensional f_0 and nonconvex f_0 , are in Appendix C.

3.1 Ergodicity and mixing of deterministic GD

Here we show numerically that the deterministic GD dynamics is not only ergodic (on foliation) but also mixing. While technically speaking the former is only the ability to maintain an invariant distribution, the latter leads to convergence to the distribution. Fig.3(a) shows that an arbitrary ensemble of initial conditions converges to approximately the rescaled Gibbs as the number of iteration increases. Fig.3(b) shows the empirical distribution of any orbit (i.e., x_0, x_1, \dots starting with an arbitrary x_0) also converges to the same limit. Fig.3(c) gives a visual that one orbit already looks 'stochastic', even though repeating the GD iteration one would get exactly the same orbit.

For the sake of length, we chose a convex but not strongly convex f_0 here. The strongly convex case was proved and will be illustrated in multi-dimension in Appendix C.3.

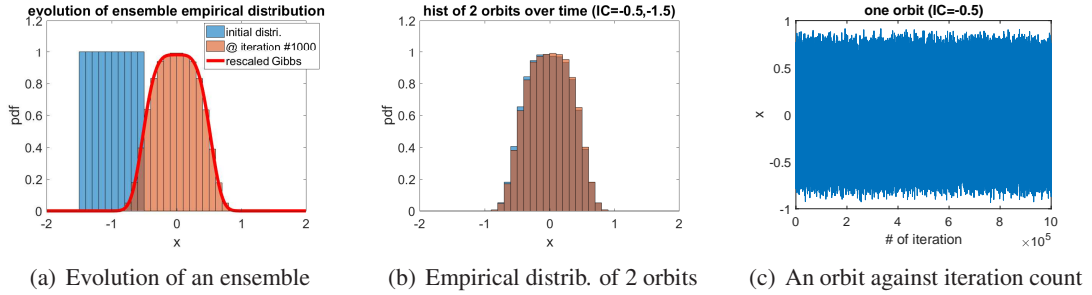


Figure 3: Ergodicity and mixing of φ . $f_0 = x^4/4$, $f_1(x) = \sin(x)$ and $\eta = 0.1, \epsilon = 10^{-6}$.

3.2 Generalization to non-periodic small scale features

Theoretical results in this paper assumed the small scale f_1 to be periodic, which may not be the case in reality. This numerical experiment shows that the stochastic behavior of deterministic GD persists even when f_1 is not periodic. This is again due to the chaotic dynamics of GD at large LR. We also note that theoretically showing local chaos (i.e., orbit filling a local potential well of $f_0 + f_{1,\epsilon}$) is relatively easy (it's mainly due to unimodal map's universality, e.g., Strogatz [2018]), but numerically observed is in fact global chaos, in which f_1 facilitates the exploration of f_0 landscape.

Here we choose $f_0 = x^2/2$ and $f_1 = \epsilon \cos(1 + \cos(\frac{\sqrt{3}}{5}x)\frac{x}{\epsilon})$, the former the simplest, and the latter an arbitrarily made-up nonperiodic microscopic function. Results are in Fig. 4.

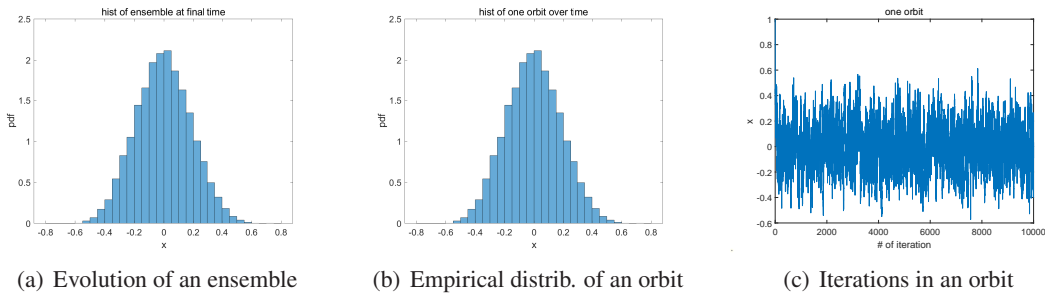


Figure 4: Ergodicity and mixing of φ for nonperiodic small scale. $\epsilon = 10^{-4}$ and $\eta = 0.1$.

3.3 What happens if momentum is added to GD?

Our theory is only for vanilla deterministic gradient decent, but we also numerically observed that deterministic GD with momentum still exhibits stochastic behaviors with large LR. Just for illustrations, consider $f_0 = x^2/2$, $f_1(x) = \sin(x)$, and two common ways for adding momentum:

3.3.1 Heavy Ball

The iteration is [Polyak, 1964]

$$v_{n+1} = \gamma y_n - \eta \nabla f(x_n), \quad x_{n+1} = x_n + v_{n+1},$$

with $v_0 = 0$. See the stochasticity of x in Fig.5.

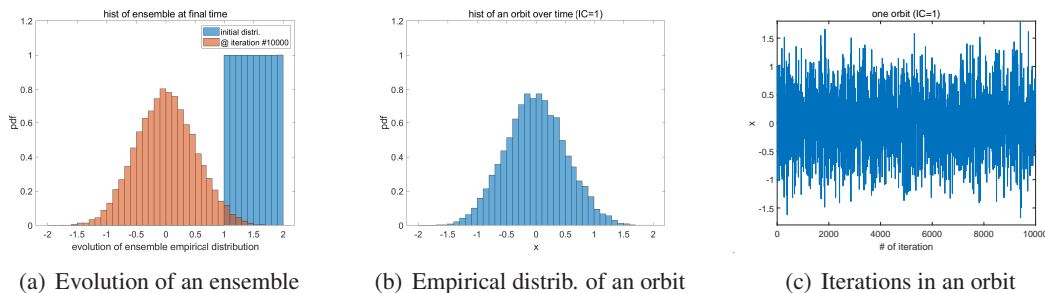


Figure 5: Heavy ball experiment. $\eta = 0.01$, $\epsilon = 0.0001$, and $\gamma = 0.9$.

3.3.2 Nesterov Accelerated Gradient for strongly convex function (NAG-SC)

The iteration is [Nesterov, 2013]

$$y_{k+1} = x_k - \eta \nabla f_0(x_k), \quad x_{k+1} = y_{k+1} + c(y_{k+1} - y_k),$$

with $y_0 = x_0$. $c = \frac{1 - \sqrt{\mu\eta}}{1 + \sqrt{\mu\eta}}$ where μ is supposed to be the strong convexity constant; we chose μ to be that for f_0 , i.e. $\mu = 1$. See the stochasticity of x in Fig. 6. The smaller variance is due a different scaling for relating η to a timestep in continuous time (see e.g., Su et al. [2014]).

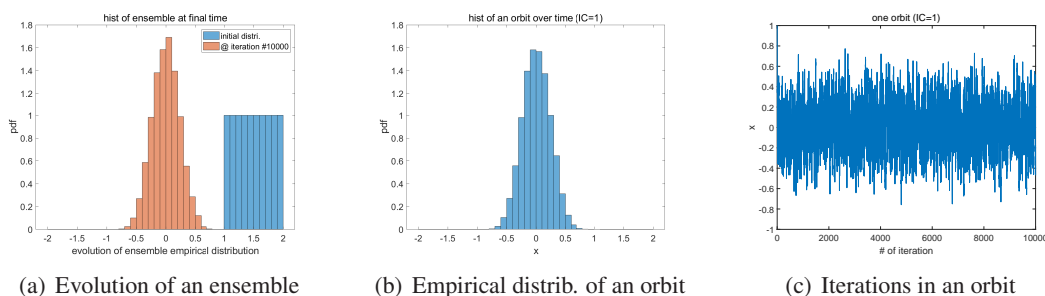


Figure 6: NAG-SC experiment. $\eta = 0.01$, $\epsilon = 0.0001$.

3.4 The case of nonconvex and multimodal f_0

Both escapes from f_0 's local minima (and the corresponding potential wells) and nonescapes are possible. Roughly speaking, this depends on how strong f_1 is when compared with f_0 . Appendix.C.4 contains detailed numerical results. Meanwhile, we note:

Remark 9. As theoretically shown, especially in section 2.3.1, 2.3.2 and 2.3.3, we see that chaos can be just a localized small-scale behavior, thus independent of the convexity of f_0 . However, the limiting distribution of the deterministic map is a global property and it should depend on the global behavior of f_0 . As will be explained in Rmk.12, when f_0 is not convex, it can happen that an orbit cannot jump between potential wells, and then unique ergodicity is lost in the sense that multiple ergodic foliations appear and respectively localize to individual potential wells. In this case, the limiting statistics is no longer unique. However, every connected subset of the support of an invariant distribution of the stochastic map can be an ergodic foliation, so if we regard the invariant distributions of the deterministic map and the stochastic map as convex combinations of the invariant distributions in each potential well, the conclusion in Theorem 4 still stands.

Acknowledgments

This research was mainly conducted when LK visited Georgia Institute of Technology. The authors thank Jacob Abernethy, Simon S. Du, Ruilin Li, Andre Wibisono, and Tuo Zhao for helpful discussions. MT was partially supported by NSF DMS-1847802 and ECCS-1936776.

References

- Zeyuan Allen-Zhu, Yuanzhi Li, and Yingyu Liang. Learning and generalization in overparameterized neural networks, going beyond two layers. In *Advances in neural information processing systems*, pages 6155–6166, 2019a.
- Zeyuan Allen-Zhu, Yuanzhi Li, and Zhao Song. A convergence theory for deep learning via over-parameterization. In *International Conference on Machine Learning*, pages 242–252, 2019b.
- Kathleen T Alligood, Tim D Sauer, and James A Yorke. Chaos: An introduction to dynamical systems. 1996, 1997.
- Sanjeev Arora, R Ge, B Neyshabur, and Y Zhang. Stronger generalization bounds for deep nets via a compression approach. In *35th International Conference on Machine Learning, ICML 2018*, 2018.
- Bernd Aulbach and Bernd Kieninger. On three definitions of chaos. *Nonlinear Dyn. Syst. Theory*, 1(1):23–37, 2001.
- Peter L Bartlett, Dylan J Foster, and Matus J Telgarsky. Spectrally-normalized margin bounds for neural networks. In *Advances in Neural Information Processing Systems*, pages 6240–6249, 2017.
- Louis S Block and William A Coppel. *Dynamics in one dimension*. Springer, 2006.
- Vivek S Borkar and Sanjoy K Mitter. A strong approximation theorem for stochastic recursive algorithms. *Journal of optimization theory and applications*, 100(3):499–513, 1999.

- Yuan Cao and Quanquan Gu. Generalization error bounds of gradient descent for learning overparameterized deep ReLU networks. *AAAI*, 2020.
- Minwoo Chae, Stephen G Walker, et al. A novel approach to bayesian consistency. *Electronic Journal of Statistics*, 11(2):4723–4745, 2017.
- Predrag Cvitanovic. *Universality in chaos*. Routledge, 2017.
- Robert Devaney. *An introduction to chaotic dynamical systems*. CRC Press, 2018.
- Laurent Dinh, Razvan Pascanu, Samy Bengio, and Yoshua Bengio. Sharp minima can generalize for deep nets. In *Proceedings of the 34th International Conference on Machine Learning-Volume 70*, pages 1019–1028. JMLR. org, 2017.
- Felix Draxler, Kambis Veschgini, Manfred Salmhofer, and Fred A Hamprecht. Essentially no barriers in neural network energy landscape. *arXiv preprint arXiv:1803.00885*, 2018.
- Simon Du, Jason Lee, Haochuan Li, Liwei Wang, and Xiyu Zhai. Gradient descent finds global minima of deep neural networks. In *International Conference on Machine Learning*, pages 1675–1685, 2019a.
- Simon S Du, Xiyu Zhai, Barnabas Poczos, and Aarti Singh. Gradient descent provably optimizes over-parameterized neural networks. *ICLR*, 2019b.
- Gintare Karolina Dziugaite and Daniel M Roy. Computing nonvacuous generalization bounds for deep (stochastic) neural networks with many more parameters than training data. *Uncertainty in Artificial Intelligence*, 2017.
- Weinan E, Chao Ma, and Lei Wu. A comparative analysis of the optimization and generalization property of two-layer neural network and random feature models under gradient descent dynamics. *Science China Mathematics*, 2020.
- J-P Eckmann and David Ruelle. Ergodic theory of chaos and strange attractors. In *The theory of chaotic attractors*, pages 273–312. Springer, 1985.
- Guilherme Franca, Daniel Robinson, and Rene Vidal. Admm and accelerated admm as continuous dynamical systems. In *International Conference on Machine Learning*, pages 1559–1567, 2018.
- Noah Golowich, Alexander Rakhlin, and Ohad Shamir. Size-independent sample complexity of neural networks. In *Conference On Learning Theory*, pages 297–299, 2018.
- Ernst Hairer, Christian Lubich, and Gerhard Wanner. *Geometric numerical integration: structure-preserving algorithms for ordinary differential equations*, volume 31. Springer Science & Business Media, 2006.
- Hubert Hennion and Loïc Hervé. Central limit theorems for iterated random lipschitz mappings. *The Annals of Probability*, 32(3):1934–1984, 2004.

- Stanisław Jastrzębski, Zachary Kenton, Devansh Arpit, Nicolas Ballas, Asja Fischer, Yoshua Bengio, and Amos Storkey. Three factors influencing minima in sgd. *arXiv preprint arXiv:1711.04623*, 2017.
- Chi Jin, Rong Ge, Praneeth Netrapalli, Sham M Kakade, and Michael I Jordan. How to escape saddle points efficiently. In *Proceedings of the 34th International Conference on Machine Learning-Volume 70*, pages 1724–1732. JMLR. org, 2017.
- Nikola B Kovachki and Andrew M Stuart. Analysis of momentum methods. *arXiv preprint arXiv:1906.04285*, 2019.
- Jason D Lee, Max Simchowitz, Michael I Jordan, and Benjamin Recht. Gradient descent only converges to minimizers. In *Conference on learning theory*, pages 1246–1257, 2016.
- Qianxiao Li, Cheng Tai, and E Weinan. Stochastic modified equations and adaptive stochastic gradient algorithms. In *International Conference on Machine Learning*, pages 2101–2110, 2017.
- Qianxiao Li, Cheng Tai, and E Weinan. Stochastic modified equations and dynamics of stochastic gradient algorithms i: Mathematical foundations. *Journal of Machine Learning Research*, 20(40):1–40, 2019a.
- Tien-Yien Li and James A Yorke. Period three implies chaos. *The American Mathematical Monthly*, 82(10):985–992, 1975.
- Xingguo Li, Junwei Lu, Zhaoran Wang, Jarvis Haupt, and Tuo Zhao. On tighter generalization bound for deep neural networks: Cnns, resnets, and beyond. *arXiv preprint arXiv:1806.05159*, 2018.
- Yuanzhi Li and Yingyu Liang. Learning overparameterized neural networks via stochastic gradient descent on structured data. In *Advances in Neural Information Processing Systems*, pages 8157–8166, 2018.
- Yuanzhi Li, Colin Wei, and Tengyu Ma. Towards explaining the regularization effect of initial large learning rate in training neural networks. In *Advances in Neural Information Processing Systems*, pages 11669–11680, 2019b.
- Yuanyuan Liu, Fanhua Shang, James Cheng, Hong Cheng, and Licheng Jiao. Accelerated first-order methods for geodesically convex optimization on Riemannian manifolds. In *Advances in Neural Information Processing Systems*, pages 4868–4877, 2017.
- Aleksandr Mikhailovich Lyapunov. The general problem of the stability of motion. *International journal of control*, 55(3):531–534, 1992.
- Yi-An Ma, Niladri Chatterji, Xiang Cheng, Nicolas Flammarion, Peter Bartlett, and Michael I Jordan. Is there an analog of Nesterov acceleration for MCMC? *arXiv preprint arXiv:1902.00996*, 2019.

- Stephan Mandt, Matthew D Hoffman, and David M Blei. Stochastic gradient descent as approximate bayesian inference. *The Journal of Machine Learning Research*, 18(1):4873–4907, 2017.
- Jürgen Moser. *Stable and random motions in dynamical systems: With special emphasis on celestial mechanics*, volume 1. Princeton University Press, 1973.
- Eric Moulines and Francis R Bach. Non-asymptotic analysis of stochastic approximation algorithms for machine learning. In *Advances in Neural Information Processing Systems*, pages 451–459, 2011.
- Yurii Nesterov. *Introductory lectures on convex optimization: A basic course*, volume 87. Springer Science & Business Media, 2013.
- Behnam Neyshabur and Zhiyuan Li. Towards understanding the role of over-parametrization in generalization of neural networks. In *International Conference on Learning Representations (ICLR)*, 2019.
- Behnam Neyshabur, Ryota Tomioka, and Nathan Srebro. Norm-based capacity control in neural networks. In *Conference on Learning Theory*, pages 1376–1401, 2015.
- Donald Ornstein and Benjamin Weiss. Geodesic flows are bernoullian. *Israel Journal of Mathematics*, 14(2):184–198, 1973.
- Valery Iustinovich Oseledec. A multiplicative ergodic theorem. liapunov characteristic number for dynamical systems. *Trans. Moscow Math. Soc.*, 19:197–231, 1968.
- Edward Ott. *Chaos in dynamical systems*. Cambridge university press, 2002.
- Grigoris Pavliotis and Andrew Stuart. *Multiscale methods: averaging and homogenization*, volume 53. Springer, 2008.
- Boris T Polyak. Some methods of speeding up the convergence of iteration methods. *USSR Computational Mathematics and Mathematical Physics*, 4(5):1–17, 1964.
- Boris T Polyak and Anatoli B Juditsky. Acceleration of stochastic approximation by averaging. *SIAM journal on control and optimization*, 30(4):838–855, 1992.
- Herbert Robbins and Sutton Monro. A stochastic approximation method. *The Annals of Mathematical Statistics*, pages 400–407, 1951.
- Nicolas L Roux, Mark Schmidt, and Francis R Bach. A stochastic gradient method with an exponential convergence rate for finite training sets. In *Advances in neural information processing systems*, pages 2663–2671, 2012.
- J. A. Sanders, F. Verhulst, and J. Murdock. *Averaging Methods in Nonlinear Dynamical Systems*. Springer, 2010.

- AN Sharkovskii. Coexistence of cycles of a continuous map of the line into itself. *International Journal of Bifurcation and Chaos*, 5(05):1263–1273, Original 1962; Translated 1995.
- Bin Shi, Simon S Du, Michael I Jordan, and Weijie J Su. Understanding the acceleration phenomenon via high-resolution differential equations. *arXiv preprint arXiv:1810.08907*, 2018.
- Yakov G Sinai. Dynamical systems with elastic reflections. *Russian Mathematical Surveys*, 25(2):137, 1970.
- Leslie N Smith. Cyclical learning rates for training neural networks. In *2017 IEEE Winter Conference on Applications of Computer Vision (WACV)*, pages 464–472. IEEE, 2017.
- Leslie N Smith and Nicholay Topin. Super-convergence: Very fast training of neural networks using large learning rates. In *Artificial Intelligence and Machine Learning for Multi-Domain Operations Applications*, volume 11006, page 1100612. International Society for Optics and Photonics, 2019.
- Steven H Strogatz. *Nonlinear dynamics and chaos: with applications to physics, biology, chemistry, and engineering*. CRC Press, 2018.
- Weijie Su, Stephen Boyd, and Emmanuel Candes. A differential equation for modeling Nesterov’s accelerated gradient method: Theory and insights. In *Advances in Neural Information Processing Systems*, pages 2510–2518, 2014.
- Molei Tao and Tomoki Ohsawa. Variational optimization on Lie groups, with examples of leading (generalized) eigenvalue problems. *International Conference on Artificial Intelligence and Statistics*, 2020.
- Colin Wei, Jason D Lee, Qiang Liu, and Tengyu Ma. Regularization matters: Generalization and optimization of neural nets vs their induced kernel. In *Advances in Neural Information Processing Systems*, pages 9709–9721, 2019.
- Andre Wibisono, Ashia C. Wilson, and Michael I. Jordan. A variational perspective on accelerated methods in optimization. *Proceedings of the National Academy of Sciences*, 113(47): E7351–E7358, 2016. ISSN 0027-8424.
- Lai-Sang Young. Statistical properties of dynamical systems with some hyperbolicity. *Annals of Mathematics*, 147:585–650, 1998.
- Tong Zhang. Solving large scale linear prediction problems using stochastic gradient descent algorithms. In *Proceedings of the twenty-first international conference on Machine learning*, page 116. ACM, 2004.

A On modified equation

As detailed in Hairer et al. [2006] Chap IX.1, in order for a discrete map

$$\Phi_\eta(x) = x + \eta g(x) \quad (\text{in our case } g(x) = f'(x) = f'_0(x) + f'_1(x/\epsilon))$$

to be the η -time flow of

$$\dot{x} = g(x) + \eta g_2(x) + \eta^2 g_3(x) + \dots, \quad (4)$$

we need

$$\begin{aligned} g_2(x) &= -\frac{1}{2!} g' g(x) \\ g_3(x) &= -\frac{1}{3!} (g''(g, g)(x) + g' g' g(x)) - \frac{1}{2!} (g' g_2(x) + g'_2 g(x)) \\ &\dots \end{aligned}$$

Note each derivative of g gives a factor of $1/\epsilon$, and thus $g_n = \mathcal{O}(\epsilon^{-(n-1)})$. Therefore, RHS of (4) diverges if $\eta \geq C\epsilon$ for some $C > 0$, in which case the more higher-order correction terms are included, the worse approximation power the modified ODE will have.

B Proofs and additional remarks

B.1 Lemmas, proofs and remarks for Thm.4

Remark 10. • We explain the purpose that we use an open set \mathcal{E} accumulating at 0 but does not use a interval such as $(0, 1]$ directly here. In the later Theorem 11, we proved that for a fixed f_0 and η , there exists periodic f_1 and arbitrary small ϵ to make the non trivial invariant distribution doesn't exist. We can use the set \mathcal{E} to eliminate this bad case that we doesn't want to see.

- About condition 3, since $\hat{\varphi}$ is continuous, and intuitively, $\hat{\varphi}$ is the limit of φ_ϵ when $\epsilon \rightarrow 0$, so the uniform equicontinuity of φ_ϵ according to ϵ is a reasonable requirement.
- In Lemma 1, we give a sufficient condition for $\hat{\Omega}$ to have a unique element, denoted as $\hat{\nu}$. When this happens, the conclusion will be $\{\nu\}_{i=1}^\infty \rightarrow \hat{\nu}$. We do numerical tests on this situation in Sec.C.3. When $\hat{\Omega}$ have multiple elements, please see related numerical test in Sec.C.4.

In order to prove Theorem 4, we need the following lemmas.

Lemma 3. $\forall \mu_0 \in \mathcal{F}, \exists \mu \in L^2(\mathbb{R}^d) \cap \mathcal{P}(\mathbb{R}^d)$, satisfying:

$$\|\mu - \mu_0\|_2 = \mathcal{O}(\epsilon) \quad (5)$$

$$\hat{\varphi}_\# \mu = \varphi_{\epsilon\#} \mu \quad (6)$$

Proof. Denote by I_U the density function of U and by $I_{\epsilon U}$ the density function of ϵU . Let $\mu := \mu_0 * I_{\epsilon U}$. It is easy to show $\|\mu - \mu_0\|_\infty = \mathcal{O}(\epsilon)$. This implies $\|\mu - \mu_0\|_2 = \mathcal{O}(\epsilon)$. Eq.5 is proved.

For eq.6, denote by X_0 the random variable with density μ_0 , then μ is the density of $X_0 + \epsilon U$ (denoted by X).

$\forall x_0$, the densities of $\varphi_\epsilon(x_0)$ and $\hat{\varphi}(x_0)$ are respectively $\int_0^T x_0 - \eta \nabla f_0(x_0) - \eta \nabla f_{1,\epsilon}(x_0 + \epsilon u) du$ and $\int_0^T x_0 - \eta \nabla f_0(x_0) - \eta \nabla f_1(u) du$.

Since $f_{1,\epsilon}$ has period ϵT and $\nabla f_{1,\epsilon}(\epsilon v) = \nabla f_1(v)$ for any v , these two densities are equal. Since this holds for any x_0 on which we condition the value of X and U is independent of X , we have $\varphi_\epsilon(X) = \hat{\varphi}(X)$ in distribution. \square

Lemma 4. *Under the conditions of Theorem 4, $\forall \{\epsilon_i\}_{i=1}^\infty \subset \mathcal{E}$ whose limit is 0, we have $\|\varphi_{\epsilon_i \#} \mu_0 - \hat{\varphi}_\# \mu_0\|_2 \rightarrow 0, \forall \mu_0 \in \mathcal{F}$ as $i \rightarrow \infty$.*

Proof. Let $\mu = \mu_0 * I_{\epsilon U}$ (as in Lemma 3), then

$$\begin{aligned} \|\varphi_{\epsilon_i \#} \mu_0 - \hat{\varphi}_\# \mu_0\|_2 &\leq \|\varphi_{\epsilon_i \#} \mu_0 - \varphi_{\epsilon_i \#} \mu\|_2 + \|\hat{\varphi}_\# \mu_0 - \hat{\varphi}_\# \mu\|_2 + \|\varphi_{\epsilon_i \#} \mu - \hat{\varphi}_\# \mu\|_2 \\ &= \|\varphi_{\epsilon_i \#} \mu_0 - \varphi_{\epsilon_i \#} \mu\|_2 + \|\hat{\varphi}_\# \mu_0 - \hat{\varphi}_\# \mu\|_2 \end{aligned}$$

Due to the uniformly equicontinuity of $\varphi_{\epsilon_i \#}$ and the continuity of $\hat{\varphi}$, both terms converge to 0 when $\epsilon \rightarrow 0$. So

$$\|\varphi_{\epsilon_i \#} \mu_0 - \hat{\varphi}_\# \mu_0\|_2 \rightarrow 0, \text{ as } i \rightarrow \infty$$

\square

Lemma 5. $\hat{\varphi}_\#(\bar{\mathcal{F}}) \subset \bar{\mathcal{F}}, \varphi_{\epsilon \#}(\bar{\mathcal{F}}) \subset \bar{\mathcal{F}}$ (The closure here is under norm $\|\cdot\|_2$). And $\bar{\mathcal{F}}$ is complete.

Proof. Because of the continuity of $\varphi_{\epsilon \#}$ for $\epsilon \in \mathcal{E}$ and $\hat{\varphi}_\#$ under $\|\cdot\|_2$, we know that $\bar{\mathcal{F}}$ is also closed under the maps $\hat{\varphi}_\#$ and $\varphi_{\epsilon \#}$. And we know the three function spaces, which are $L^2(\mathbb{R}^d), \mathcal{P}(\mathbb{R}^d)$ and $L_{\mathcal{F}}$ -Lipschitz continuous functions are all complete, so their intersection is also complete under $\|\cdot\|_2$. \square

This lemma prepares us to use Arzela-Ascoli lemma in the following proof.

Proof of Thm.4. Suppose $\varphi_{\epsilon_i \#} \nu_i = \nu_i$. Let $i \rightarrow +\infty$, according to Lemma 4, we have

$$\|\varphi_{\epsilon_i \#} \nu_i - \hat{\varphi}_\# \nu_i\|_2 \rightarrow 0$$

$$\|\nu_i - \hat{\varphi}_\# \nu_i\|_2 \rightarrow 0$$

Since $\bar{\mathcal{F}}$ consists of L^2 bounded and $L_{\mathcal{F}}$ -Lipschitz continuous functions that are also non-negative and integrating to 1, it is a subset of L^∞ . This is because if $\mu \in \bar{\mathcal{F}}$ is not bounded, then because of Lipschitz continuity, the integral of μ will diverge.

Because $\bar{\mathcal{F}}$ is a closed set in a complete space (Lemma 5), Arzela-Ascoli lemma guarantees that $\{\nu_i\}_{i=1}^\infty$ has at 1 subsequence that converges uniformly and denote by ν_0 the limit of one of such subsequence. Since $\hat{\varphi}$ is continuous under $\|\cdot\|_2$, ν_0 satisfies $\hat{\varphi}_\# \nu_0 = \nu_0$, so we have $\nu_0 = \hat{\nu}$, so we proved all the limit of $\{\nu_i\}_{i=1}^\infty$ is in $\hat{\Omega}$. \square

B.2 On the stochastic map $\hat{\varphi}$

B.2.1 Some quantitative results about its ergodicity

Proof of Lemma 1. Here we use the machinery provided by Hennion and Hervé [2004]. Regard $\hat{\varphi}$ as a random action on \mathbb{R}^d . In this proof, we write the dependence of $\hat{\varphi}$ on ζ explicitly as $\hat{\varphi}_\zeta$. Choose a fixed point x_0 and let

$$\begin{aligned} c(\zeta) &:= \sup \left\{ \frac{d(\hat{\varphi}_\zeta x, \hat{\varphi}_\zeta y)}{d(x, y)} : x, y \in \mathbb{R}^d, x \neq y \right\} \\ \mathcal{M}_{\gamma+1} &:= \int_G (1 + c(\zeta) + d(\varphi_\zeta x_0, x_0))^\gamma d\pi(\zeta) \\ \mathcal{C}_{\gamma+1}^{(n_0)} &:= \int_G c(\varphi_\zeta) \max\{c(\varphi_\zeta), i\}^\gamma d\pi^{*n}(\zeta) \end{aligned}$$

In $\hat{\varphi}$ and the our interested chaotic regime of learning rate, since f_0 is strongly convex and L -smooth, we choose η_0 small to ensure $c(\varphi_\zeta) = \max_{x \in \mathbb{R}^d} \|I - \eta_0 \text{Hess} f_0(x)\|_2 < 1$, and we choose $\gamma = 0$, $n_0 = 1$ to get $\mathcal{M}_{\gamma+1} = E_\zeta[1 + c(\varphi_\zeta) + d(\hat{\varphi}_\zeta(x_0), x_0)] < +\infty$ and $\mathcal{C}_{\gamma+1}^{(1)} = E_\zeta[c(\varphi_\zeta)] < 1$.

Under these facts, Theorem 1 in Hennion and Hervé [2004] ensures that there is a unique $\hat{\varphi}$ -invariant probability distribution $\hat{\mu}_0$. Moreover, geometric ergodicity holds in the Prokhorov distance d_P . Namely, there exists positive real number C and $\kappa_0 < 1$, such that, for any probability distribution μ on M satisfying $\mu(d(\cdot, x_0)) < +\infty$, and all $n \geq 1$,

$$d_P(\hat{\varphi}_\#^{(n)} \mu, \hat{\mu}_0) \leq C \kappa_0^{n/2}$$

□

Remark 11. In a separable metric space, which is our case, convergence of measures in the Prokhorov metric is equivalent to weak convergence of measures, which is also equivalent to the convergence of cumulative distribution functions.

The following two remarks show that convexity and L -smoothness of f_0 are necessary for geometric ergodicity established by Lemma 1.

Remark 12. Here we will explain in 1-dim, what can happen when the function f_0 is not convex. Since the random variable ζ is bounded, denote it by $[a, b]$. Unlike in a standard overdamped Langevin case, there can be potential barriers in f_0 that $\hat{\varphi}$ cannot cross, because the noise is of a finite strength. To make this quantitative, we assume the existence of an invariant distribution with density μ_0 , and calculate what kind of points are not in the support of μ_0 . When $\eta < 1/L$, for a point $x \in \text{supp} \hat{\mu}_0$, we have $\eta f'_0(x) \in \eta[a, b]$. So if $\{x | f'_0(x) \in [a, b]\}$ is not a connected set (note that it is independent from η), then the support of the invariant density will be separated in to disjoint components, and no orbit can jump between them. An example explains why the set can be disconnected:

Suppose $f_0 = k(x^2 - 1)^2$, $k > 0$ for example, and $f_1 = \sin(x)$. Calculate the set $S := \{x : f'_0(x) \in [-1, 1]\} = \{x : |4kx(x^2 - 1)| < 1\}$. We have that when $k < \frac{3\sqrt{3}}{8}$, S is connected. But

when $k > \frac{3\sqrt{3}}{8}$, the set S is not connected. In this case, a point cannot jump from one well to another as $\hat{\varphi}$ is closed in each connected component of S , which means ergodicity on S is lost. Which distribution the system converges to (if existent) relies on which well the initial condition belongs to.

In multi-dimension case, connectedness is different from simply connectedness, which complicates the intuition. We won't discuss it here.

See also Rmk. 9 on jumping between potential wells by the deterministic map.

Remark 13. When f_0 is not L -smooth, such as $f_0(x) = (x^2 + 1)^2$ and $f_1 = \sin(x)$. For a fixed η , it is easy to see that when the absolute value of initial condition is greater than x_0 , where x_0 is the greatest solution of $x - 4\eta x(x^2 + 1) + \eta + x = 0$, we know $P(|\hat{\varphi}(x)| > |x|) = 1$, so the system will explode and never converge to any distribution. This is because $\mathcal{M}_{\gamma+1} < \infty$ in the proof of Lemma 1 is not satisfied.

Theorem 9 (coupling estimation of the exponential convergence rate of $\hat{\varphi}$). *Consider the iteration $x_{k+1} = x_k - \eta \nabla f_0(x_k) + \eta \zeta_k$ for i.i.d. $\zeta_k = -\nabla f_1(U_k)$. Assume x_0 has continuous density and f_0, f_1 are C^1 , and denote by ρ_k the density of x_k . If f_0 is μ -strongly convex, then the limiting distribution ρ_∞ exists and the 2-Wasserstein distance satisfies the nonasymptotic bound*

$$W_2(\rho_k, \rho_\infty) \leq (1 - 2\eta\mu)^{k/2} C \quad (7)$$

for some constant $C \geq 0$.

Proof. Existence of ρ_∞ is guaranteed by Lemma 1.

Let \hat{x}_0 be a random variable distributed according to ρ_∞ and define

$$\hat{x}_{k+1} = \hat{x}_k - \eta \nabla f_0(\hat{x}_k) + \eta \zeta_k$$

using the same noise ζ_k .

Let $d_k := x_k - \hat{x}_k$, then

$$d_{k+1} = d_k - \eta (\nabla f_0(x_k) - \nabla f_0(\hat{x}_k))$$

Therefore,

$$\begin{aligned} \|d_{k+1}\|^2 &= \|d_k\|^2 - 2\eta \langle d_k, \nabla f_0(x_k) - \nabla f_0(\hat{x}_k) \rangle + \eta^2 \|\nabla f_0(x_k) - \nabla f_0(\hat{x}_k)\|^2 \\ &\leq \|d_k\|^2 - 2\eta\mu \|d_k\|^2 \leq (1 - 2\eta\mu) \|d_k\|^2. \end{aligned}$$

The second last inequality is because strong convexity implies quadratic gradient growth. Thus,

$$\mathbb{E}\|x_{k+1} - \hat{x}_{k+1}\|^2 \leq (1 - 2\eta\mu)^k \mathbb{E}\|x_0 - \hat{x}_0\|^2$$

Note \hat{x}_k is distributed according to ρ_∞ because that is the invariant distribution and $\hat{x}_0 \sim \rho_\infty$. By definition,

$$\begin{aligned} W_2(\rho_k, \rho_\infty)^2 &= \inf_{\pi \in \Pi(\rho_k, \rho_\infty)} \int \|y_1 - y_2\|^2 d\pi(y_1, y_2) \\ &\leq \mathbb{E}\|x_k - \hat{x}_k\|^2. \end{aligned}$$

Therefore, the choice of $C = \mathbb{E}\|x_0 - \hat{x}_0\|^2$ leads to eq.7. \square

Corollary 1 (Spectral gap of $\hat{\varphi}$ is at least at the order of η). *Consider the setup of Thm.9 and $\eta \leq \frac{1}{2\mu}$. Denote by L the transition operator of the Markov process generated by $\hat{\varphi}$, i.e., $L\rho_k = \rho_{k+1} \quad \forall k$. Then L has a single eigenvalue of 1, and any other eigenvalue λ satisfies $|1 - \lambda| \geq \eta\mu$.*

Proof. Since $\hat{\varphi}$ generates a Markov process, any eigenvalue has modulus bounded by 1.

The single eigenvalue of 1 is guaranteed by geometric ergodicity (Lemma 1). Thus, for any other eigenvalue λ , $|\lambda| < 1$.

Let ρ_{\perp} be the eigenfunction corresponding to λ . Since L preserves the normalization of probability density, $\int \rho_{\perp} = 0$.

For any $\alpha \neq 0$, let x_0 be a random variable distributed according to density $\rho_{\infty} + \alpha\rho_{\perp}$. We have

$$\rho_{x_k} = L^k(\rho_{\infty} + \alpha\rho_{\perp}) = \rho_{\infty} + \alpha\lambda^k\rho_{\perp}$$

and therefore the L_1 distance satisfies

$$d_1(\rho_{x_k}, \rho_{\infty}) = \alpha\lambda^k\|\rho_{\perp}\|_1$$

Since densities exist, we have the total variation distance

$$d_{TV}(\rho_{x_k}, \rho_{\infty}) = \frac{1}{2}d_1(\rho_{x_k}, \rho_{\infty}) = \frac{1}{2}\alpha\|\rho_{\perp}\|_1\lambda^k$$

Although in general total variation distance cannot be upper bounded by Wasserstein distance, it was shown in Chae et al. [2017] Lemma 5.1 that such an upper bound exists when both probability distributions admit smooth densities, i.e.,

$$d_{TV}(\rho_{x_k}, \rho_{\infty}) \leq CW_2(\rho_{x_k}, \rho_{\infty})$$

for some $C \geq 0$. Combined with Thm. 9, this thus gives

$$d_{TV}(\rho_{x_k}, \rho_{\infty}) \leq \hat{C}\sqrt{1 - 2\eta\mu}^k \leq \hat{C}(1 - \eta\mu)^k$$

for some $\hat{C} \geq 0$. Therefore, $|\lambda| \leq 1 - \eta\mu$. This leads to $|1 - \lambda| \geq \eta\mu$. \square

B.2.2 On Proposition 1

To prove this bound, we first prove Lemma 2:

Proof of Lemma 2.

$$\begin{aligned} \mathbb{E}\|\nabla f_0(X_0)\|_2^2 &= \frac{1}{Z_1} \int \|\nabla f_0(x)\|_2^2 \exp\left(-\frac{2f_0(x)}{\eta}\right) dx \\ &\leq \frac{\sqrt[k]{\eta}}{Z_2} \int \|\nabla f_0(x)\|_2^2 \exp\left(-2C_1\left(\frac{\|x\|}{\sqrt[k]{\eta}}\right)^{k_1}\right) d\frac{x}{\sqrt[k]{\eta}} \\ &= \frac{\sqrt[k_1]{\eta}}{Z_2} \int \|\nabla f_0(\sqrt[k_1]{\eta}u)\|_2^2 \exp(-2C_1\|u\|^{k_1}) du \end{aligned}$$

Since $\|f_0(x_0) - f_0(x)\| > C_2\|x - x_0\|^{k_2}$, we have

$$\frac{\|\nabla f_0(x) - \nabla f_0(x_0)\|}{\|x - x_0\|^{k_2-1}} < C_2$$

So

$$\begin{aligned} \mathbb{E}\|\nabla f_0(Y_0)\|_2^2 &= \frac{\sqrt[k_1]{\eta}}{Z_4} \int C_2(\sqrt[k_1]{\eta}\|u\|)^{2(k_2-1)} \exp(-2C_1\|u\|^{k_1}) du \\ &= \eta^{2k_2-2-\frac{1}{k_1}} \frac{1}{Z_4} \int C_2\|u\|^{2(k_2-1)} \exp(-2C_1\|u\|^{k_1}) du \end{aligned}$$

The integral converges and is a constant, so we have

$$\mathbb{E}\|\nabla f_0(X_0)\|_2^2 = \mathcal{O}(\eta^{2k_2-2-\frac{1}{k_1}})$$

□

Proof of Prop. 1. Because $\tilde{\zeta}$ is compactly supported and $\|\nabla f_0\|$ is bounded, Taylor expansion of h in η gives, $\forall X$,

$$\begin{aligned} \mathbb{E}(h(\hat{\varphi}(X))) &= \mathbb{E}_X \left[\mathbb{E}_{\tilde{\zeta}}[h(X - \eta\nabla f_0(X) + \eta\tilde{\zeta})|X] \right] \\ &= \mathbb{E}_X h(X - \eta\nabla f_0(X)) + \eta \mathbb{E}_{\tilde{\zeta}}^\top \mathbb{E}_X [\nabla h(X - \eta\nabla f_0(X))] \\ &\quad + \frac{\eta^2}{2} \mathbb{E}_X \left[\mathbb{E}_{\tilde{\zeta}}[\tilde{\zeta}^\top \text{Hess}h(X - \eta\nabla f_0(X))\tilde{\zeta}|X] \right] + \mathcal{O}(\eta^3) \\ &= \mathbb{E}_X \left[h(X) - \eta\nabla f_0(X)^\top \cdot \nabla h(X) + \frac{\eta^2}{2} \nabla f_0(X)^\top \text{Hess}h(X) \nabla f_0(X) + \frac{\eta^2}{2} \mathbb{E}_{\tilde{\zeta}}^\top \text{Hess}h(X) \mathbb{E}_{\tilde{\zeta}} \right] + \mathcal{O}(\eta^3) \end{aligned}$$

When $X = X_0$, we first estimate the 3rd term. Since $\text{Hess}h$ is bounded and due to the L -smoothness and strong convexity of f_0 , we know it is $\mathcal{O}(\eta^3)$ using Lemma 2 in the case $k_1 = k_2 = 2$. So we get

$$\mathbb{E}(h(\hat{\varphi}(X_0))) - \mathbb{E}h(X_0) = \frac{\eta^2}{2Z} \int \left[-\frac{2}{\eta} \nabla f_0(x)^\top \cdot \nabla h(x) + \sigma^2 \text{Tr} \text{Hess}h(x) \right] \exp\left(-\frac{2f_0(x)}{\eta\sigma^2}\right) dx + \mathcal{O}(\eta^3)$$

And then we use Stokes' theorem to prove the integration in RHS vanishes. Denote

$$\omega := \sum_i (-1)^i \nabla_i h(x) \exp\left(-\frac{2f_0(x)}{\eta\sigma^2}\right) dx_1 \wedge \dots \wedge \widehat{dx}_i \wedge \dots \wedge dx_n$$

where \widehat{dx}_i means dropout dx_i . Then

$$\begin{aligned} d\omega &= \sum_i \nabla_i^2 h(x) \exp\left(-\frac{2f_0(x)}{\eta\sigma^2}\right) - \frac{2}{\eta\sigma^2} \nabla_i h(x) \nabla_i f_0(x) \exp\left(-\frac{2f_0(x)}{\eta\sigma^2}\right) dx_1 \wedge \dots \wedge dx_n \\ &= (\text{tr} \text{Hess}h - \frac{2}{\eta\sigma^2} \nabla h^\top \cdot \nabla f_0) \exp\left(-\frac{2f_0(x)}{\eta\sigma^2}\right) dx_1 \wedge \dots \wedge dx_n \end{aligned}$$

According Stokes' formula,

$$\begin{aligned}\mathbb{E}(h(\hat{\varphi}(X))) - \mathbb{E}h(X) &= \frac{\eta^2 \sigma^2}{2Z} \int_{\mathbb{R}^d} d\omega + \mathcal{O}(\eta^3) \\ &= \frac{\eta^2 \sigma^2}{2Z} \lim_{r \rightarrow \infty} \int_{B(0,r)} d\omega + \mathcal{O}(\eta^3) \\ &= \frac{\eta^2 \sigma^2}{2Z} \lim_{r \rightarrow \infty} \int_{\partial B(0,r)} \omega + \mathcal{O}(\eta^3)\end{aligned}$$

The first term vanishes since $h(x)$ is compactly supported, which gives us the conclusion that

$$\mathbb{E}(h(\hat{\varphi}(X_0))) - \mathbb{E}h(X_0) = \mathcal{O}(\eta^3)$$

□

B.2.3 On Theorem 5

Proof. Consider a deviation function

$$r := \rho_\infty - \tilde{\rho}.$$

Decompose r as an orthogonal sum

$$r = r_1 + r_0 \quad \text{where } r_1 \in \ker(I - L) \text{ and } r_0 \perp \ker(I - L)$$

Since $\hat{\varphi}$ induces a geometric ergodic process, $\dim \ker(I - L) = 1$, and thus

$$r = \gamma \rho_\infty + r_0 \quad \text{for some scalar } \gamma.$$

Since $L\rho_\infty = \rho_\infty$ and $L\tilde{\rho} = \tilde{\rho} + \mathcal{O}(\eta^3)$ (Prop.1; note weak-* topology is metrizable on a separable space), we have $(I - L)r = \mathcal{O}(\eta^3)$, and consequently

$$(I - L)r_0 = \mathcal{O}(\eta^3)$$

Since r_0 is orthogonal to $\ker(I - L)$ which is the eigenspace associated with eigenvalue 1 of L , and all eigenvalues of $I - L$, except for the irrelevant 0, satisfy $|\lambda| \geq \mu\eta$ due to Cor.1, we obtain

$$r_0 = \mathcal{O}(\eta^2).$$

This means $\rho_\infty - \tilde{\rho} = \gamma \rho_\infty + \mathcal{O}(\eta^2)$. Since ρ_∞ and $\tilde{\rho}$ are both density functions that normalize to 1, applying a uniform test function and letting its support go to infinity give $0 = \gamma + \mathcal{O}(\eta^2)$. This yields eq.2. □

Remark 14. The invariant distribution can be approximated by not only rescaled Gibbs but a Gaussian if f_0 is strongly convex. Here is the intuition of a more general result:

Consider rescaled Gibbs (1). Due to the small η at the denominator, X_0 assumes small values with exponentially large probability. We thus can formally Taylor expand $f_0(x)$ about $x = 0$,

which we assumed WLOG to be the minimizer. Denote the first nonzero derivative of f_0 at 0 by the k th one. Then $f_0(x) \approx \frac{1}{k!} f_0^k(0) x^k$. So, from the density of rescaled Gibbs, we see the density of $\frac{X_0}{\sqrt[k]{\eta}}$ can be approximated by

$$\frac{X_0}{\sqrt[k]{\eta}} \sim \frac{1}{Z} \exp\left(\frac{-2f_0^k(0)}{k!\sigma^2} x^k\right)$$

Note that iff f_0 is strongly convex, $k = 2$, and one gets a Gaussian approximation.

Remark 15. If one considers another stochastic map $\tilde{\varphi}(x) := x - \eta \nabla f_0(x) + \eta \sigma \xi$ where ξ is standard i.i.d. Gaussian, $\tilde{\varphi}(x)$ admits, under the same Lipschitz and convexity conditions, a similar limiting invariant distribution $\frac{1}{Z} \exp\left(-\frac{2f_0(x)}{\eta\sigma^2}\right)$ will be obtained. The key difference is, unlike $\tilde{\varphi}$ which uses unbounded noise and is the discretization of an SDE, our stochastic map $\hat{\varphi}$ uses only bounded noise as it mimicks the deterministic map φ .

B.3 On the deterministic map φ

B.3.1 Li-Yorke Chaos

Remark 16. About Thm.6, see Sharkovskii [Original 1962; Translated 1995], Li and Yorke [1975] for rigorous theorems and proofs. This is one of the most celebrated result in chaotic dynamics, which tells us that period 3 implies chaos. The 1st conclusion is named after Sharkovskii. The 2nd conclusion in this theorem is also generalized to be the definition of Li-Yorke Chaos in multi-dim case.

B.3.2 Counter examples

Theorem 10 (a sufficient condition for the nonexistence of nondegenerate invariant distribution). *When $d = 1$, for any fixed ϵ and fixed periodic $f_1 \in C^2(\mathbb{R})$, for any η_0 , there exists $\eta > \eta_0$ and $f_0 \in C^2$ such that $|f_0'|$ and $|f_0''|$ (but 3-order or more derivative will explode) are arbitrarily small. For such f_0 , the orbit starting at any point is bounded but φ does not admit a nontrivial invariant distribution.*

Proof.

$$\varphi'(x) = 1 - \eta f_0''(x) - \frac{\eta}{\epsilon} f_1''\left(\frac{x}{\epsilon}\right)$$

Because of the continuity of f_1'' , $1 - \frac{\eta}{\epsilon} f_1''(\frac{x}{\epsilon})$ has a zero point, denote as x_0 . So we can choose δ to make $\frac{1 - \eta/\epsilon f_1''(x/\epsilon)}{\eta}$ arbitrarily small on the interval $I = [x_0 - \delta, x_0 + \delta]$. Then construct $f_0|_I$ and η making $\varphi' \equiv 0$ on I . After that, we adjust f_0 to make $\varphi(x_0)$, which is not in I , be a fixed point of φ . According to the property of Li-Yorke chaos, all the point will be finally mapped to I , and then to $\varphi(x_0)$ and never move. So the nontrivial invariant distribution does not exist. \square

Theorem 11 (another sufficient condition for the nonexistence of invariant distribution). *When $d = 1$, \forall fixed $f_0 \in C^2$ and $\eta > 0$, there exists periodic $f_1 \in C^2$ whose period is 1 and 0,1,2-order derivative is arbitrary small, together with an ϵ arbitrarily small, making nontrivial invariant distribution not exist.*

Proof. Choose f_1 s.t. $\nabla^2 f_1(\frac{x}{\epsilon}) \equiv \frac{\epsilon}{\eta}(1 - \eta \nabla^2 f_0(x))$ on a interval $[0, \delta]$ where $\delta \ll \epsilon$ and make f_1 and f_1' arbitrarily small on $[0, \delta/\epsilon]$, and choose f_1 on $[\delta/\epsilon]$ to ensure continuity and smoothness. We can make $\epsilon \rightarrow 0$ to make f_1'' small. Then choose a specific ϵ to make $\varphi(0)$ is a fix point. According to the property of Li-Yorke chaos, all the point will be finally mapped to $[0, \delta]$, then to $\varphi(0)$ and never move. So the nontrivial invariant distribution does not exist. \square

Remark 17. The requirements for η to be arbitrarily large in Theorem 10 and ϵ to be arbitrarily small in Theorem 11 ensure the system won't converge to a local minimum created by f_1 , and from the construction of the counterexamples, we know the system is not the other trivial one, which means the system explodes because η is too large.

Remark 18. Here we give some intuition of Thm.10 and 11. Thm.6 tells us that in 1-dim case, if we have a period-3 orbit, then there exists a subset S of the whole space J satisfying: For every $x_1, x_2 \in S$ with $x_1 \neq x_2$, $\liminf_{n \rightarrow \infty} |\varphi^{(n)}(x_1) - \varphi^{(n)}(x_2)| = 0$. So the intuition for proving Thm. 10 and 11 is to make $\varphi \equiv 0$ on a small interval, then all the points that drop in this interval will be mapped to a single fixed point of φ .

B.3.3 On Theorem 7

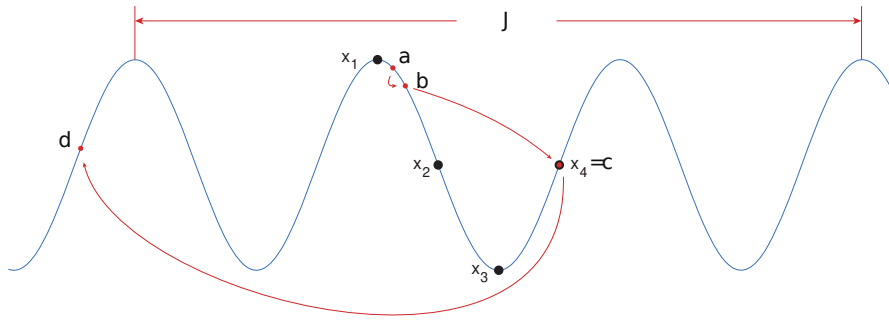


Figure 7: Guideline to finding a period-3 orbit

Proof. We follow the intuition illustrated in Fig.7. Denote the stationary point of f_0 by x , i.e. $f_0'(x) = 0$. Then since f_1 is nonconstant, differentiable and essentially defined on a compact set, we have $\inf\{f_1'\} < f_0'(x) < \sup\{f_1'\}$ and $f_0 \in \mathcal{C}^1$. So there exists a interval $J = [x - \delta, x + \delta]$ s.t. $\inf\{f_1'\} < f_0'(x) < \sup\{f_1'\}$ on J . So when $3\epsilon T < 2\delta$, there must exists $x_1, x_2, x_3, x_4 \in J$, satisfying $x_1 < x_2 < x_3 < x_4$, $x_4 - x_1 < \epsilon T$ and $\varphi(x_1) = x_1, \varphi(x_2) > x_2, \varphi(x_3) = x_3, \varphi(x_4) < x_4$.

Because of the continuity of f_0 , x_2 and x_4 above can be chosen to satisfy $\varphi_\epsilon(x_2) - x_2 = \eta(\sup(f_1') - f_0'(x))$ and $\varphi_\epsilon(x_4) - x_4 = \eta(\inf f_1' - f_0'(x))$.

Let $c = x_4$, and $d = \varphi(c)$. Let ϵ be small to satisfy $\varphi_\epsilon(x_4) - x_4 < -\epsilon T$ and $\epsilon T < \varphi(x_2) - x_2$. So we have $\varphi(x_2) > c$. And since $\varphi(x_1) = x_1$ and continuity, $b \in [x_1, x_2]$ s.t. $\varphi(b) = c$. By the same way we get $a \in [x_1, b]$ s.t. $\varphi(a) = b$. Based on Thm.6, we deduct that the discrete dynamical system induced by φ is chaotic in Li-Yorke sense. \square

B.3.4 On the Lyapunov exponent

Proof of Thm.8. All the norms for matrix in this proof is 2-norm. For simplicity, we omit the footnote.

Denoted by ν the invariant distribution of the deterministic map. Denote the special map where is $f_0 = 0$ as φ_0 :

$$\varphi_0(x) = x - \eta \nabla f_{1,\epsilon}(x)$$

With ergodicity, when $\epsilon \rightarrow 0$, we have

$$\begin{aligned} \lambda(x) &= \lim_{n \rightarrow \infty} \frac{1}{n} \sum_{i=1}^n \ln \|\nabla \varphi|_{\varphi^{(i)}(x)}\| \\ &= \int \ln \|\nabla \varphi|_x\| \nu(dx) \\ &= \int \ln \|\nabla \varphi_0|_x + \eta \text{Hess} f_0(x)\| \nu(dx) \end{aligned}$$

Since $\text{Hess} f_0$ is bounded, we know that

$$\lambda(x) = \int \ln \|\nabla \varphi_0|_x\| \nu(dx) + \mathcal{O}(\eta)$$

And then we divide the support of the invariant distribution into small parts according to the period of $\epsilon f_1(x/\epsilon)$, and enumerate them with $A_j, j \in \mathbb{N}$.

$$\begin{aligned} \lambda(x) &= \sum_i \int_{A_j} \ln \|\nabla \varphi|_x\| \nu(dx) + \mathcal{O}(\eta) \\ &= \sum_i \int_{A_j} \frac{1}{\epsilon |\Gamma|} \left(\int_{\epsilon \Gamma} \ln \|\nabla^2 f_{1,\epsilon}(y)\| dy + \mathcal{O}(\epsilon) \right) \nu(dx) + \mathcal{O}(\eta) \\ &= \ln \left(\frac{\eta}{\epsilon} \right) + \frac{1}{|\Gamma|} \int_{\Gamma} \ln \|\nabla^2 f_1(y)\| dy + \mathcal{O}(\epsilon + \eta) \end{aligned}$$

□

Remark 19. Here we need φ to be ergodic, which means the distribution of a single trajectory converges to the invariant distribution of the chaotic dynamical system. We don't have a reference, but please see section 3.1 for numerical test.

C More numerical evidence

C.1 Period doubling

We illustrate numerically that φ , when viewed as a family of maps indexed by LR η , keeps undergoing period doubling bifurcation as η increases, and the period of η eventually approaches infinite at a finite η value, which is the chaos threshold (e.g., Alligood et al. [1997], Chap 11). This observation is rather robust to f_0 , and we choose a convex but not strongly-convex example for an illustration.

The bifurcation diagram is plotted in Fig.8. For each η value, we start with a fixed initial condition and iterate it using GD dynamics (φ) for sufficiently long so that the dynamics settle into an attractor, and then draw each of the thereafter iterations as a point on the diagram. For example, one can read from Fig.8 that there are two points at $\eta = 2.5\epsilon$, corresponding to an orbit of period 2. Although limited by the numerical resolution, one can see that the chaos threshold in this case is around $\eta \approx 3.5\epsilon$.

Worth mentioning is that the chaos that first onsets is a local one, happening in a (and every) small potential well created by $f_{1,\epsilon}$. In other words, before global chaos for which LR is so large that GD can escape local well, arbitrarily large period already appears and chaos already onsets. This can be seen from Fig.8 as the boundaries of a small potential well, which is approximately $[-\epsilon\pi, \epsilon\pi]$, are marked by red dashed lines.

C.2 Lyapunov exponent

Thm.8 provides a quantitative estimate of the Lyapunov exponent of the deterministic GD map φ . Although we did require an additional strong convexity condition on f_0 for the geometric ergodicity of the stochastic map $\hat{\varphi}$, our results about the deterministic map do not have this requirement.

As an illustration, we pick multimodal nonconvex $f_0 = (x^2 - 1)^2$, together with $f_{1,\epsilon}(x) = \epsilon \sin\left(\frac{x}{\epsilon}\right)$. Fig.'s 9 and 10 respectively plot how the numerically computed Lyapunov exponent depends on η (with fixed ϵ) and on ϵ (with fixed η). The constant $m \approx \lambda(x) - \ln(\eta/\epsilon)$ is around 0.7 in both plots, which agrees with our theoretical estimate of $m = \frac{1}{2\pi} \int_0^{2\pi} \ln |\sin(y)| dy \approx -0.6931$.

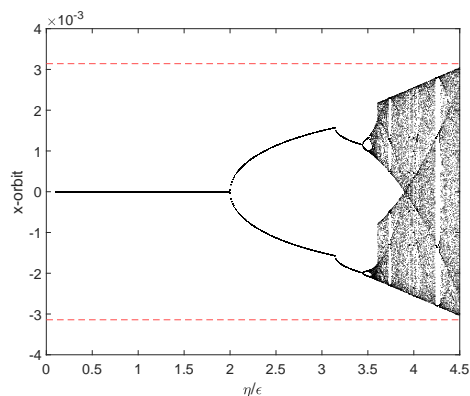


Figure 8: Bifurcation diagram of deterministic GD with $\epsilon = 10^{-3}$, $f_0 = x^4/4$ and $f_1 = -\cos(x)$.

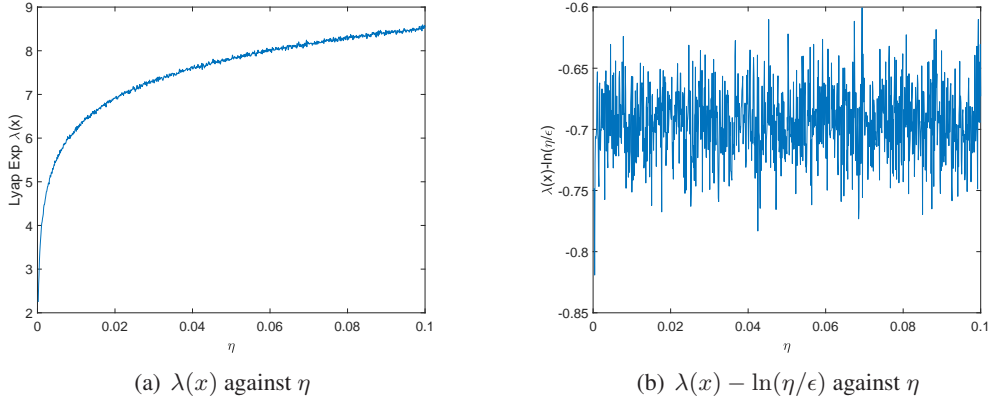


Figure 9: Dependence of the Lyapunov exponent on η

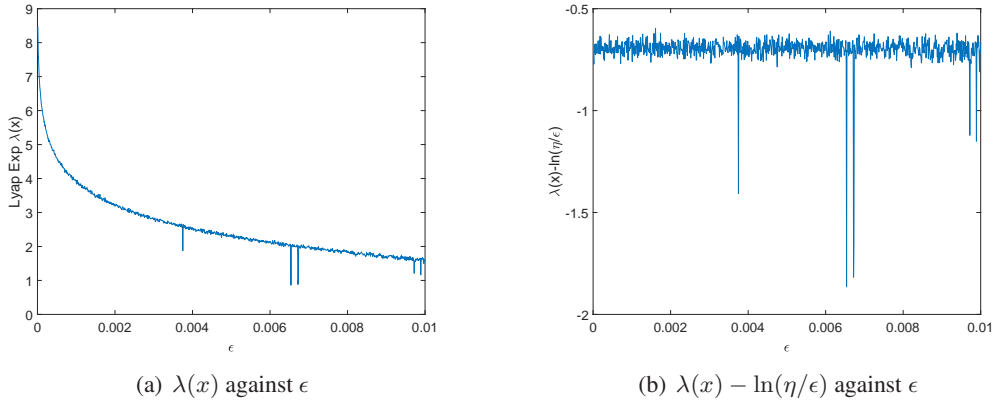


Figure 10: Dependence of the Lyapunov exponent on ϵ

C.3 A multidimensional demonstration

Our sufficient condition for chaos (Thm.7) is restricted to 1D problems, although our connection between φ and $\hat{\varphi}$ limiting statistics (Sec.2.1) and the approximation of $\hat{\varphi}$ limiting statistics (Sec.2.2) work for any finite dimension. We conjecture that stochasticity also appears in large LR GD for multidimensional multiscale objective functions. A numerical experiment consistent with this conjecture is presented, based on a classical strongly convex test function of Matyas:

Let f_0 be defined as

$$f_0(x, y) = 0.26(x^2 + y^2) + 0.48xy.$$

The small scale is arbitrarily chosen to be

$$f_{1,\epsilon}(x, y) = \epsilon \sin(x/\epsilon) + \epsilon \cos(y/\epsilon), \epsilon = 10^{-7}.$$

The evolution of the empirical distribution of an ensemble, respectively under GD φ and the stochastic map $\hat{\varphi}$, is shown in Fig.11, where good agreement is observed. The GD empirical distribution is also compared with rescaled Gibbs in Fig.12, where results again agree.

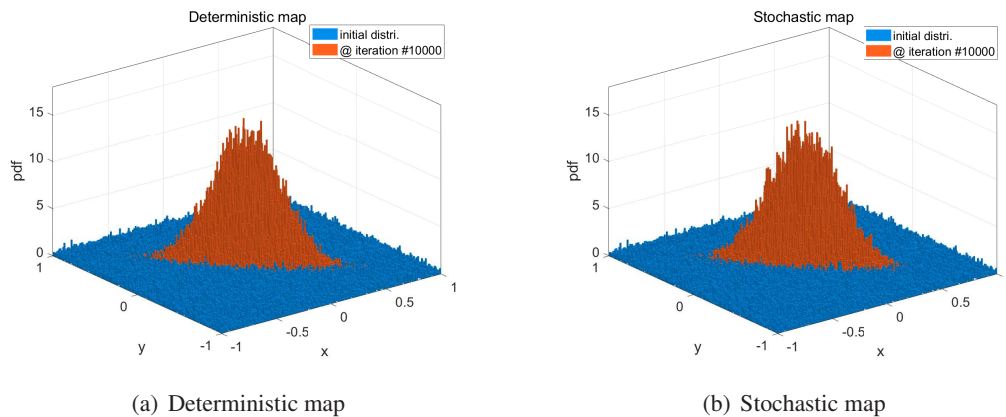


Figure 11: Comparison between the deterministic map and the stochastic map on Matyas function ($\eta = 0.01$) for testing Thm.4. Agreed histograms suggests that the limiting distributions of the two maps are close.

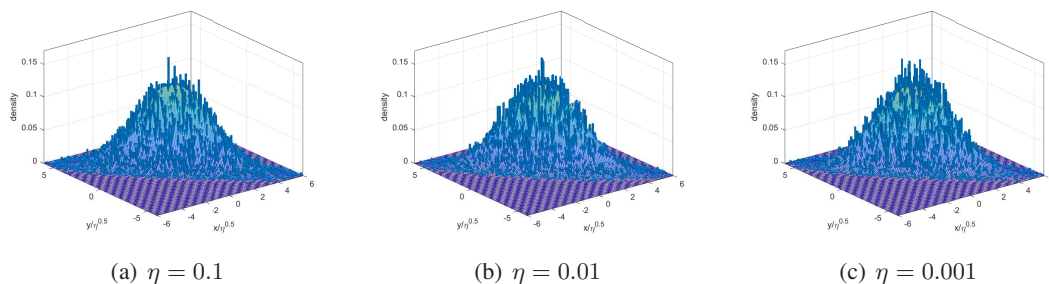


Figure 12: Test for the explicit expression of the invariant distribution. The surface is rescaled Gibbs and the histogram is the experiment result. They are overplotted after a rescaling by $\sqrt{\eta}$ in both axis. Observed agreement is consistent with the rescaled Gibbs approximation.

In terms of deterministic chaos, although our sufficient condition for chaos (Thm.7) is only for 1-dim., the Lyapunov exponent estimate (Thm.8) works for any finite dimension as it assumes already ergodicity. Here we observe numerically that the deterministic map is chaotic and mixing (thus ergodic) despite of the ≥ 2 dimension: see Fig.13 for the statistical behavior of a single orbit. A comparison with Fig.11 gives agreement in the statistics.

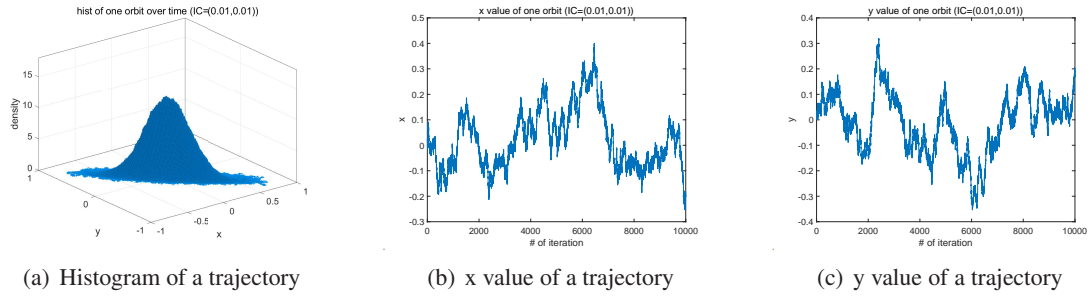


Figure 13: The histogram of a single trajectory. We can see that it is the same as the experimental result for the invariant distribution in Fig.11(b).

Then we numerically calculate the Lyapunov exponent. We chose a random initial point, run sufficiently many iterations, and use eq.3 to compute it. At the same time, Thm.8 gives a theoretical estimation, with $m = \frac{1}{4\pi^2} \int_{[0,2\pi]^2} \ln \max(|\sin(x)|, |\cos(y)|) dx dy \approx -0.2669$. Fig.'s 14 and 15 show that this estimation, namely $\lambda(x) \approx m + \ln(\frac{\eta}{\epsilon})$, is again correct up to $\mathcal{O}(\epsilon + \eta)$ error.

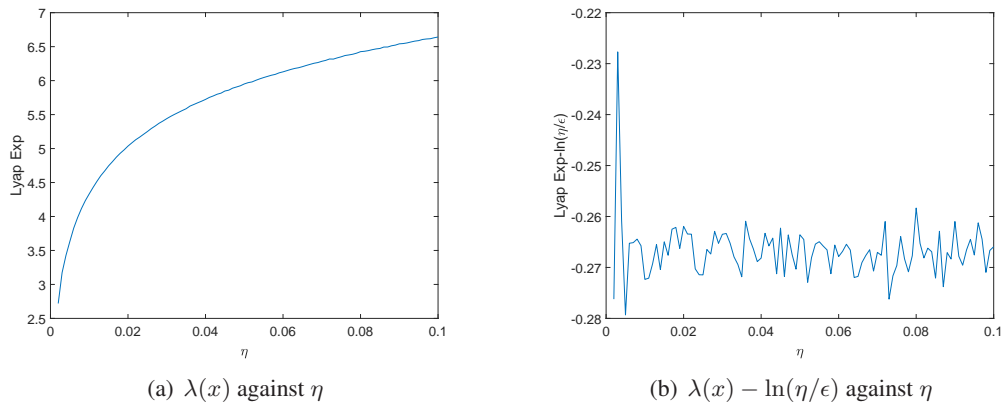


Figure 14: Dependence of $\lambda(x)$ on η ($\epsilon = 0.00001$)

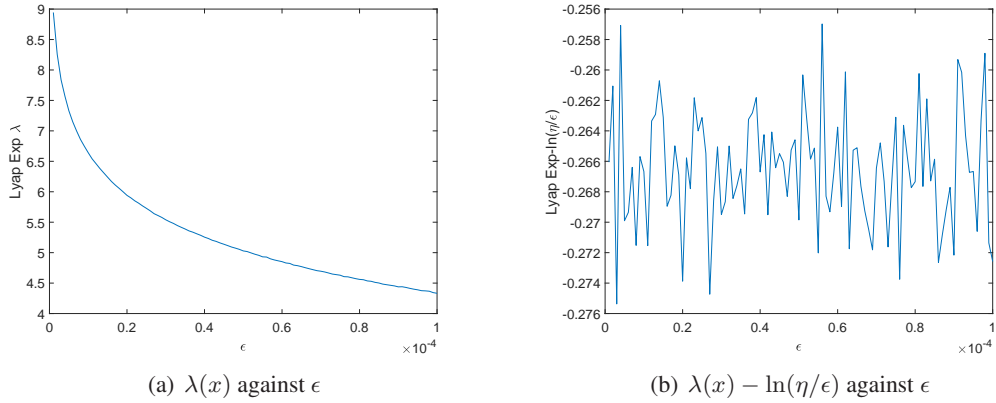
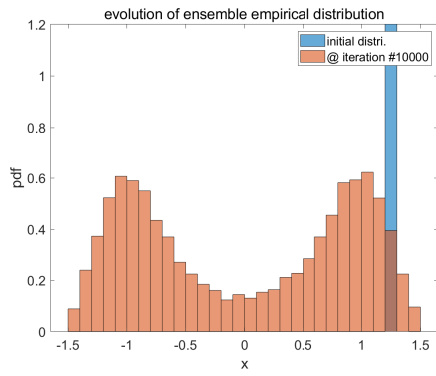


Figure 15: Dependence of $\lambda(x)$ on ϵ ($\eta = 0.1$)

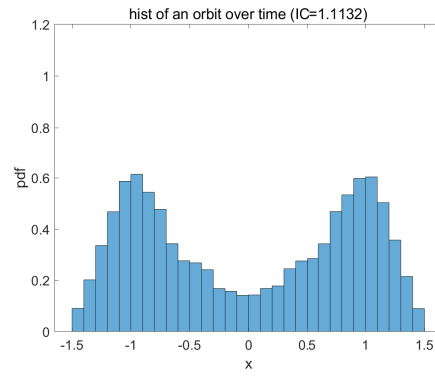
C.4 The nonconvex f_0 dichotomy: to escape or not to escape macroscopic potential well created by f_0 ?

What will happen when there are several potential wells in the landscape of f_0 ? Rmk.9 and 12 already provided some discussions and now we'll demonstrate two possible outcomes concretely in numerical experiments. We will use the same test function, which is $f_0(x) = k(x^2 - 1)^2$ and $f_1(x) = \sin(x)$. $x > 0$ and $x < 0$ are two potential wells of f_0 .

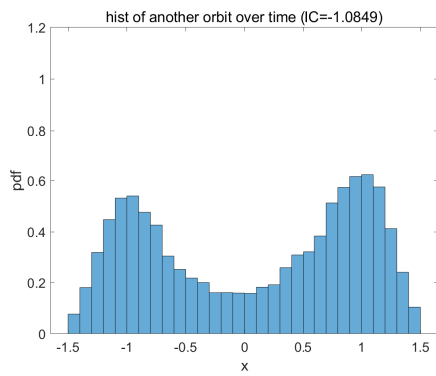
We already obtained a bound on the relative strength between f_0 and f_1 ; it is $k_{critical} = \frac{3\sqrt{3}}{8}$ for whether the point can jump from one potential well to another. Fig.'s 16 and 17 respectively illustrates the long-time statistics of GD when $k = 0.05 < k_{critical}$ and $k = 5 < k_{critical}$. Results are consistent with theoretical predictions.



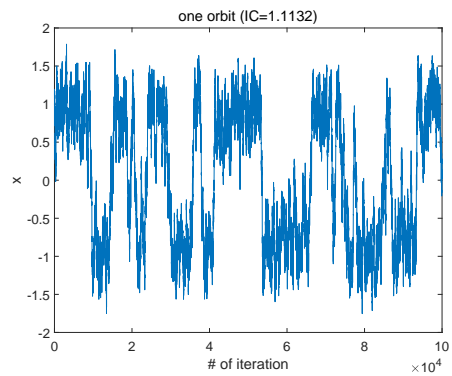
(a) Invariant distribution



(b) Histogram of a trajectory

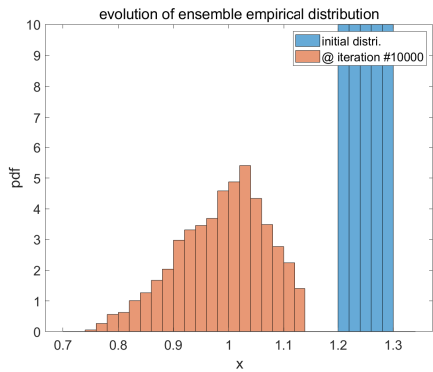


(c) Histogram of another trajectory

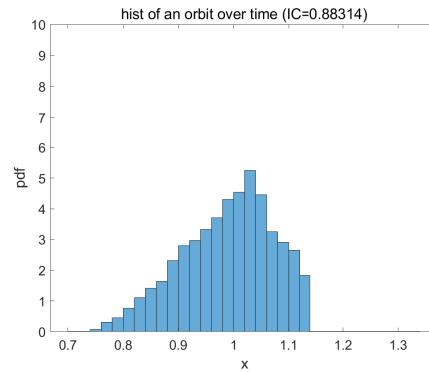


(d) One trajectory

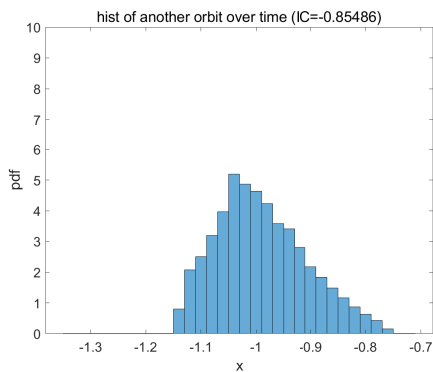
Figure 16: A non-convex mixing example. The initial condition is concentrated in the right potential well but barrier crossing happens. $k = 0.02$, $\eta = 0.05$ and $\epsilon = 0.0001$.



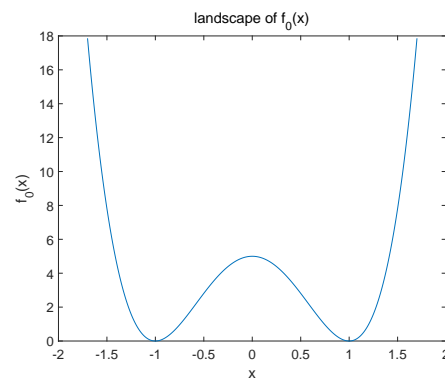
(a) One of the invariant distributions



(b) Histogram of a trajectory, starting in the right well



(c) Histogram of another trajectory, starting in the left well



(d) Landscape of f_0

Figure 17: A non-convex and non-mixing example. The initial condition is concentrated in the right potential well but no orbit can cross the potential barrier at $x = 0$. There is at least another invariant distribution in the left potential well due to symmetry. But if one restricts to the foliation within the potential well, convergence to a statistical limit still occurs. $k = 5$, $\eta = 0.05$ and $\epsilon = 0.0001$.

Interestingly, we observe that Rmk.14 still holds even though the orbit is confined in one potential well if k is large. As $f''(1) > 0$, the function is strongly convex in a neighborhood of $x = 1$, and rescaled Gibbs can be approximated by a Gaussian density of $\exp(-16k(x-1)^2)/Z$. Fig.18 shows that the ensemble empirical distribution indeed converges to this prediction as $\eta \rightarrow 0$.

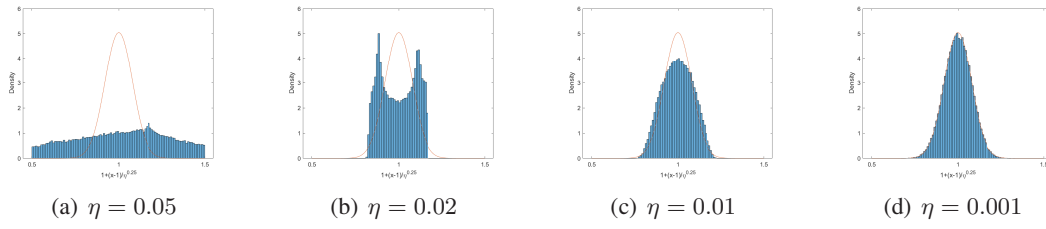


Figure 18: Empirical distributions of a sufficiently evolved ensemble for different η values when $k = 5$. The red line is the theoretical approximation in Rmk.14. Note x-axis has been zoomed in via $x \mapsto 1 + (x - 1)/\sqrt{\eta}$ for focusing on the essential part.